Fall 2016

Bioresponsive polymer coating on nanoparticles

Tunyaboon Laemthong

Department:

BIORESPONSIVE POLYMER COATING ON NANOPARTICLES

by

TUNYABOON LAEMTHONG

A THESIS

Presented to the Faculty of the Graduate Faculty of the

MISSOURI UNIVERSITY OF SCIENCE AND TECHNOLOGY

In Partial Fulfilment of the Requirements for the Degree

MASTER OF SCIENCE IN CHEMICAL ENGINEERING

2016

Approved by

Sutapa Barua, Advisor
Daniel Forciniti
Yue-Wern Huang

PUBLICATION THESIS OPTION

This thesis is formatted to Missouri University of Science and Technology specifications and consists of the following two articles that have been submitted for publication as follows:

Paper I, Pages 9-40 have been submitted to NANOTECHNOLOGY

Paper II, Pages 41-51 are intended for submission in BBA GENERAL SUBJECTS

ABSTRACT

Nanotechnology incorporated with molecular biology became a promising way to treat cancer. The size of nanoparticles enables them to overcome the side effects noticed in cancer treatment like chemotherapy and surgery. Various types and shapes of nanoparticles have been synthesized and used in drug delivery to tumor sites. However, one of problems of using these nanoparticles is the aggregation after injecting them into human body due to flow rate of bloodstream. The coagulation and aggregation will result in clogging blood vessel and lower therapeutic efficacy.

In this thesis, a solution to the aggregation problem was proposed, which is coating biopolymer on nanoparticles (NPs). The experimental sections covered synthesis and characterization of breast cancer specific targeting drug-encapsulated NPs and biopolymer coating on the surface of Au-Fe_3O_4 NPs for thermal therapy. Furthermore, *in vitro* studies of these NPs with breast cancer cells were also included. The specific targeting anticancer drug-encapsulated NRs showed significant inhibition in BT-474 breast cancer cell growth. The Au-Fe_3O_4 NPs has a possibility to treat cancer cells using the thermal therapy approach.

ACKNOWLEDGMENTS

First of all, I would like to express my deepest gratitude to my advisor, Dr. Sutapa Barua, for her guidance, time and patience to provide me a great time doing the research. This research work would not have completed without her intellectual insight and constructive criticism. It has been an honor to be her student.

Also, I would like to thank Dr. Daniel Forciniti and Dr. Yue-Wern Huang for their guidance and valuable discussion through the research. I would like to thank all of the lab members who encouraged me through hard time during the research.

I am grateful to my sponsor, the Royal Thai government, for funding and the wonderful opportunity to pursue this degree.

Last, I would like to thank my family for their encouragement, support and unconditional love throughout my life.

TABLE OF CONTENTS

Page

LIST OF ILLUSTRATORS

Page

PAPER I

PAPER II

LIST OF TABLES

Page

PAPER I

SECTION

1. INTRODUCTION

Invasive diseases like cancer have been a major issue for public health. The current cancerous treatment methods such as chemotherapy or surgery still have side effects that can cause some troubles to patients.[1] Nano-biotechnology, which is the combination of nanotechnology and biology, has become a promising way to treat cancer. Many types of the particles within the nano-scale were synthesized through various methods. Among all the synthetic methods that have been used, there is still a challenge for these nanoparticles. For nanoparticles less than 100 nm in size, the long-range force between nanoparticles is controlled by Brownian motion, which causes the collision of particles and leads them to aggregation.[2] A solution to this problem is surface modification including coating something on the surface of particles. Coating biocompatible polymer on the particles is an interesting technique to help increase the potential of the nanoparticles, including anticancer drugs. It does not only increase the potential of the synthesized nanoparticles, but also helps reduce the side effects from the drug. Anticancer drugs themselves are considered highly toxic to cells. Therefore, specific targeting nanoparticles play an important role in treatment to avoid the side effects to other cells. Coating polymer on the drug may decrease toxicity and provide a surface for biomolecules like antibodies to conjugate on, which would lead to the specific targeting treatment.

Apart from polymer-coated anticancer drug nanoparticles, the gold nanoparticles were also used to study the hyperthermia induced treatment using the principal of thermal therapy. One of the promising multifunctional magnetic nanomaterials is the gold magnetite (Au-Fe_3O_4) nanoparticles. The magnetite nanoparticles have shown the ability

for biomedical applications in magnetic resonance imaging and hyperthermia induced treatment which eventually leads to cell apoptosis. Although the gold nanoparticles were found useful to treat cancer, there is still a drawback in this strategy: low retention time in the bloodstream, which caused the particle aggregation and clog blood vessel. To overcome this disadvantage, coating polymer on the surface of gold nanoparticles may increase the retention time by preventing aggregation. Therefore, this research outlines the synthesis, characterization of anticancer drug encapsulated nanoparticles, the conjugation with biomolecules on nanoparticles, the coating of biocompatible polymer on gold nanoparticles, and *in vitro* study with breast cancer cells.

1.1. BIODEGRADABLE POLYMER-COATED PARTICLES FOR CANCER TREATMENTS

1.1.1. Polycaprolactone (PCL). PCL is a synthetic biodegradable polymer.[3] It is a semi-crystalline, hydrophobic polymer in which the crystallinity decreases when molecular weight increases. Due to its properties, PCL has attracted much attention for biomedical applications.[4]

Ortiz *et al*. studied the combination of gene therapy and drug encapsulation was expected to increase the potential of the therapy. In addition, the biodegradable polymer like PCL has an ability to protect antitumor drugs from rapid elimination during *in vivo* studies. The combination of cytosine deaminase/5-fluorocytosine (CD/5-FC) and herpes simplex virus thymidine kinase (HSV-tk) was used in colon cancer therapy. The 5-FU drug encapsulated nanoparticles were prepared using the solvent emulsion method. From the results, the nanoparticles have a spherical shape with diameter of 140 ± 20 nm. Zeta potential values also indicated that the drug was entrapped within the nanoparticles. The

drug encapsulated nanoparticles were then tested *in vitro* drug release which showed a drug release profile of up to 27% within three hours of the study in neutral pH. The rapid drug release resulted from the leakage of the polymer surface in nanoparticles. From *in vivo* study, the 5-FU drug inhibited the cell proliferation in a dose-dependent manner. The combination of the 5-FU drug and E gene was investigated to study the cytotoxicity in SW480 colon cancer cells. The result showed that this combination increases the percentage of apoptotic in cells within 24 hours (83% ± 4.6%), which is greater than the independent 5-FU loaded nanoparticles (22% ± 2.5%) and E gene (41% ± 5%). Therefore, this study reveals a new strategy for colon cancer using the combination of drug-encapsulated nanoparticles and gene therapy which is a promising *in vitro* study. However, it needs to have more evidence *in vivo.*[5]

1.1.2. Poly (Lactic-Co-Glycolic Acid) (PLGA). PLGA is a copolymer, which is the combination of polylactic acid (PLA) and polyglycolic acid (PGA). It is soluble with a wide range of solvents such as tetrahydrofuran, ethylacetate, acetone.[6]

Farazuddin *et al*. used PLGA microsphere to entrap Perillyl alcohol (POH), which was reported as anti-cytotoxic properties against many types of cancer. The POH-encapsulated PLGA microparticles were synthesized using the oil-in-water based emulsion solvent method. The microparticles were characterized using SEM, which revealed the microparticle size of 768 ± 215 nm. The microparticles were further studied during *in vitro* released kinetics. After 168 hours, the overall drug release was about 30%. From an *in vitro* cytotoxicity experiment, the results indicated that the IC_{50} value of POH loaded microparticles was higher than the drug alone. In order to confirm the efficiency of the microparticles, they were tested *in vivo* using skin cancer cells. The free form of the drug

was used to compare to the drug - encapsulated microparticles. Within 13 weeks, the survival rate of the sample treated with microparticles was ~80%; meanwhile, the sample treated with the POH drug alone showed only 40% survival rate. This whole study indicated that the drug encapsulated microparticles were successfully synthesized and provided higher efficiency than the free formed drug.[7]

Verderio *et al*. used PLGA nanoparticles to encapsulate the antitumor drug curcumin (CUR). CUR has an ability to inhibit carcinogenesis at three stages: tumor promotion, angiogenesis, and tumor growth. CUR interacts with TrxR, which is overexpressed in tumor cells. TrxR is converted by NADPH oxidase and H_2O_2 is increased, which finally causes the cancer cell death. However, CUR is a hydrophobic drug. In order to overcome the problem of extremely rapid metabolism and poor absorption of CUR, this drug needs the carrier to bring it to the tumor site. CUR was encapsulated within PLGA nanoparticles using the solvent evaporation method. Drug - encapsulated nanoparticles were obtained after the centrifugation. The drug-loaded nanoparticles were characterized by TEM and SEM. The drug-encapsulated nanoparticles have a spherical shape with a diameter of 128.37 ± 6.7 nm. The amount of CUR was calculated using UV-vis and fluorescence spectroscopy, which showed about 80% encapsulation in the nanoparticles. The drug-loaded PLGA nanoparticles were further used *in vitro* with MCF7, the $HER2^+$ breast cancer cells. The CUR alone was used as a control. The results indicated that after incubating MCF7 with nanoparticles for 24 hours, 50 µg/ml of nanoparticles efficiently inhibited the tumor growth.[8]

1.1.3. Polylactic Acid (PLA). PLA is a thermoplastic polymer that has high strength and high modulus. PLA is in the group of aliphatic polyester polymers.[9] It is also

degradable through the hydrolysis of ester bond where the hydrolysis rate depends on the size and shape of particles.[10]

Zhu *et al*. used PLA to encapsulate the docetaxel (DTC) for liver cancer treatment. The aim of this study is to enhance the drug delivery to targeted tumor sites. The drug-encapsulated nanoparticles were prepared using the solvent evaporation method. Tocopherol polyethylene glycol 1000 succinate (TPGS), a water-soluble derivative of vitamin E, was used as an emulsifier in order to increase the drug encapsulation due to its bulky structure and large surface area. After removing the solvent, the surface of the drug encapsulated nanoparticles were further coated with polydopamine and then conjugated with galactosamine to specifically target liver cancer cells. After the characterization, the diameter of sphere-shaped NPs is ~ 209 nm. The nanoparticles were tested for DTC release and the result showed that at the initial stage the drug released up to 30% within 2 days of the observation. After 14 days, the cumulative DTC released was ~60%. The IC_{50} value of NPs was obtained from the cell viability, which showed that NPs were ~7 fold higher than non-targeting NPs. From *in vivo* results, the Gal-pD-TPGS-PLA NPs could reach the targeted tumor site and also inhibit the tumor growth in the liver more efficiently than non-targeting nanoparticles. The overall results gave a promising strategy for liver cancer therapy.[11]

In the study of PLA for breast cancer drug delivery, Jiang *et al*. used PLA incorporated with TPGS to form the nanoparticles. The anticancer drug used in the study was doxorubicin (DOX). The photosensitizer was used to induce endolysosome escape of the delivery system to reverse the drug resistance and overcome the co-delivery problem. This study proposed the combination of chemo-photodynamic therapy for DOX-resistant

human breast adenocarcinoma cells (MCF-7/ADR cells). The nanoparticles were prepared using the nanoprecipitation method which, resulted in sphere-shaped nanoparticles with a diameter of 140.3 ± 13.45 nm. The surface of the nanoparticles was modified by conjugating with tLyp-1 peptide .The nanoparticles were then tested *in vitro* drug release, which showed that 70% of DOX was released at pH 5.5 within 96 hours of the study. After using the laser as a trigger of the treatment, the percentage of apoptosis of nanoparticles gave the highest percentage of other samples. The result from the *in vivo* study also confirmed that the tLyp-1-NPs with the laser can inhibit the tumor growth in the mice model more efficiently than using no laser and the non-treated mice.[12]

1.1.4. Dextran. Dextran is one of the polysaccharide groups which consists of repeated monosaccharide units linked by glycosidic bonds. Dextran has been used for particles preparation because of its nonionic charges.[13]

Zhang *et al*. proposed the use of dextran conjugated with doxorubicin in order to improve low drug efficiency and side effects to overcome the multidrug resistance. Dox was conjugated on the dextran via hydrazone bonds. The selective targeting was also used in the study by grafting folate acid on dextran. The size of nanoparticles was ~148 nm in diameter. The nanoparticles were tested for drug release *in vitro* at pH 5.0, which showed DOX release up to 92% within 48 hours. The nanoparticles were further tested for cell cytotoxicity in HepG2/DOX cells. The results indicated that the folate ligand on the prodrugs had a selective targeting ability towards cells that express the folate receptor. These nanoparticles were then tested *in vivo* and the results showed that the targeted drug-capsulated nanoparticles could expand the life of treated mice and they also had fewer side effects to the heart.[14]

1.1.5. Gelatin. Gelatin is a polymer that is not only biodegradable, and biocompatible, but it also bio-adhesive properties. These important properties indicate that gelatin is a material that can easily form film and particles for biomedical applications.[15]

Lu *et al*. studied paclitaxel-loaded gelatin nanoparticles for intravesicle chemotherapy, which provides selectively drug delivery at high concentrations to tumor-bearing bladders while minimizing exposure time in the system. Paclitaxel was chosen because of its lipophilicity, which provides the ability to penetrate the urothelium more effectively than other drugs. However, entrapping paclitaxel in micelles resulted in lowering the drug concentration into the bladder tissue. The solutions to overcome this problem are using a surface active agent which is capable of disrupting the micelle structure and increasing the free fraction of paclitaxel. The drug-encapsulated gelatin nanoparticles were synthesized using the desolvation method. The size of nanoparticles was in the range of 600-1,000 nm. These nanoparticles were able to release the paclitaxel ~92% within two hours. The nanoparticles can be degraded consistently by protease. The drug-encapsulated nanoparticles can inhibit 60% of RT4 cells in 48 hours and its IC_{50} was lower than free formed drug, which showed higher efficiency in inhibiting the growth of cancer cells and was confirmed by the same trend *in vivo*.[16]

Li *et al*. studied the use of gelatin for encapsulating both hydrophobic CUR and hydrophilic DOX for dual targeting HER2-overexpressing breast cancer. The nanoparticles were synthesized using a surfactant-free method utilizing amifostine to stably link a targeting ligand (Herceptin) to amphiphilic gelatin (AG)-iron oxide-calcium phosphate (CaP) nanoparticles with hydrophobic CUR and hydrophilic DOX encapsulated in the AG core and CaP shell (AGIO-CaP-CD), respectively. Gelatin entrapped the hydrophobic

molecules by using an emulsion method. The nanoparticles were ~200 nm in diameter. After 24 hours, DOX showed fast release (~ 60% with pH 5.0) but slow release (~ 10% with pH 7.4), which means the nanoparticles were able to inhibit the premature DOX release before reaching the targeted tumor site. The drug-encapsulated nanoparticles were further tested with SK-BR-3 cells, which showed that the drug-encapsulated nanoparticles were more effective than the drug alone and gelatin can be used as a degradation controllable material.[17]

1.2. RESEARCH PROBLEM

In the context of the previous section topic, it can be said that the biodegradable polymers are useful for drug delivery in terms of drug degradation protection, drug encapsulation, and particle forming. The research problem for this thesis is to propose the method to coat the anticancer drug nanoparticles and Au-Fe_3O_4 nanoparticles in order to prevent them from coagulation and aggregation. Additionally, to help increase the potential of therapeutic efficacy for delivering nanoparticles for cancer therapy. The upcoming chapters deal with the experimental setup and their results.

PAPER

I. BIORESPONSIVE POLYMER COATING ON TARGETED DRUG NANORODS

Tunyaboon Laemthong,[a] Kelly Dunlap,[a] Caitlin Brocker,[a] Dipak Barua,[a] Daniel Forciniti,[a]

Yue-Wern Huang,[b] and Sutapa Barua [a,1]

[a] Department of Chemical and Biochemical Engineering

Missouri University of Science and Technology, Rolla, MO 65409

[b] Department of Biological Sciences

Missouri University of Science and Technology, Rolla, MO 65409

[1] To whom correspondence should be addressed. Email: baruas@mst.edu. Department of Chemical & Biochemical Engineering, 110 Bertelsmeyer Hall, 1101 N. State Street, Rolla, MO 65409-1230

ABSTRACT

Ineffective drug release at the target site is among the top challenges for cancer treatment. The first challenge reflects the fact that interactions with carriers (*i.e.*, nanoparticles) can denature the active ingredients of drugs by shear stress. The second challenge is low drug release in the disease microenvironment. Here, we report a one-step process to prepare bioresponsive polymer coated drug nanorods (NRs) from liquid precursors using the solvent diffusion method. A thin layer (10.3 ± 1.4 nm) of poly(ε-caprolactone) (PCL) polymer coating was deposited on the surface of camptothecin (CPT) anti-cancer drug NRs. The mean size of PCL-coated CPT NRs was 500.9 ± 91.3 nm length x 122.7 ± 10.1 nm width. The PCL polymer coating was biodegradable at acidic pH 6 as determined by Fourier Transform Infrared (FT-IR) spectroscopy. CPT drugs were released up to 51.5% when PCL coating dissolved into non-toxic carboxyl and hydroxyl groups. Trastuzumab (TTZ), a humanized IgG monoclonal antibody, was conjugated to the NR surface for breast cancer cell targeting. Combination treatments using CPT and TTZ decreased the HER-2 positive BT-474 breast cancer cells by 66.9 ± 5.3 % *in vitro*. These results suggest effective combination treatments of breast cancer cells using bioresponsive polymer coated drug delivery.

KEYWORDS: Anti-cancer drugs, Bioresponsive polymer coating, Breast cancer, Combination treatments, Drug nanorods, Trastuzumab

1. INTRODUCTION

Protection of molecular structures of drugs is required in order to retain its active groups and therapeutic efficiency. For example, the lactone ring of CPT drugs is converted to carboxylate form, which possesses high affinity to human serum albumin (HSA) at physiological pH 7.4, and is preferentially eliminated from the body.[1,2] Encapsulation of CPT inside polymer nanoparticles prevents the conversion of CPT into the inactive carboxylate form during blood circulation, thus increasing its likelihood of reaching the target site.[3-6] CPT has been conjugated with a variety of polymers such as β-cyclodextrin,[7,8] N-hydropropylmethacrylamide (HPMA),[9] polylactide (PLA),[10] polyethylene glycol (PEG) and polymethcryloyloxyethyl phosphoryl choline (polyMPC)[11] to improve efficacy. There are other formulations such as liposomes consisting of floxuridine and CPT-analog irinotecan,[12] and micelles comprising of CPT derivative SN38.[13] The nanostructured derivatives of CPT increase systemic exposure to CPT and anti-cancer activity in patients; however, the side effects are diarrhea, hepatic toxicity and renal failure.[14,15] In addition, most nanoparticle-drug conjugates suffer from aggregation with hydrophilic and hydrophobic backbone of nanoparticles,[16] and, therefore, low drug release.

In contrast, in the present work, we have developed a method to coat a bioresponsive polymer on elongated drug NRs. While conventional nanoparticles are made of lipids, metals and polymers, we prepared rod-shape nanoparticles using pure anti-cancer drugs, and deposited a thin layer (10.3 ± 1.4 nm) of bioresponsive polymer coating on drug NRs. Recent studies have shown that NRs enhance drug delivery as reflected in improved blood circulation time,[17] specific receptor binding[18] and cellular internalization by target cells.[18] Theoretical models and in vivo biodistribution studies support these experimental

outcomes.[17,19,20] Cationic cross-linked PEG hydrogel NRs are internalized by HeLa cells more rapidly than symmetrical shaped NPs.[21] Mesoporous silica NRs of 450 nm length are taken up more rapidly than 250 nm rods or 100 nm spherical particles by A375 human melanoma cells.[22] Rod-shaped particles can avoid phagocytosis depending on the initial contact angle to the macrophages.[23] The adhesion strength of non-spherical particles towards the blood vessel wall is higher than spherical NPs, as shown in both experimental setting, and theoretical modeling.[19,24-28] Accordingly, we prepared drug NRs in this work. We used the solvent diffusion method to prepare CPT NRs of 500.9 ± 91.3 x 122.7 ±10.1 nm size in large quantities.[29]

We encapsulate CPT drug NRs with a bioresponsive polymer, PCL. This polymer is a FDA-approved biodegradable aliphatic polyester, and is well-known for hydrolytic cleavage of ester groups, and its non-toxicity.[30] Nanoparticles composed of PCL polymer have been shown to exhibit increased blood circulation time, and reduced clearance by reticuloendothelial system (RES).[31] PCL microspheres loaded with bovine serum albumin (BSA) protein released up to 60.5% of BSA in vitro.[32] CPT, Doxorubicin and Taxol-loaded PCL microspheres efficiently released the loaded drugs from microspheres that resulted in a higher degree of cancer cell growth inhibition than free drugs.[33-35] One drawback of these polymer-drug conjugates is drug's aggregation with polymers,[16] and, therefore, low drug release. To overcome these issues, we introduce a simple and rapid technique of interfacial polymer deposition on the surface of pure drug NRs in large quantities. The significance of our systems is that the NP shape provides greater contact surface area than conventional spherical NPs, and thus, ensures greater receptor ligand interactions for binding.[36] We hypothesize that depositing a thin layer of PCL polymer on the surface of drug NRs would

not only protect drugs from degradation but also allow release of drugs at the target site due to specific receptor binding. We deposit a PCL coating from liquid precursors surrounding CPT NRs simultaneously during the drug NR formation.

Our nanocarrier system aims at selective breast cancer cell targeting by human epidermal growth factor 2 (HER-2) protein specific antibody conjugation. TTZ (Herceptin; Genentech) monoclonal antibody (mAb) binds to HER-2 overexpressed at the cell membrane by many cancer cells, including breast cancer cells.[37] It is shown that TTZ-conjugated polystyrene NRs accumulate in breast cancer cells by multivalent interactions with HER-2 receptors.[26] TTZ reduces proliferation of breast cancer cells by binding to the extracellular domain of HER-2 receptors, preventing HER-2 dimerization, and thereby inducing subsequent cell cycle arrest in G1.[38] In this study, we simultaneously delivered CPT and TTZ drugs using PCL coated NRs to achieve synergistic inhibition effects on breast cancer growth at low concentrations.

2. MATERIALS AND METHODS

2.1 SYNTHESIS OF PCL POLYMER COATED CPT NRs

All reagents were purchased from Sigma-Aldrich unless otherwise specified. We deposited a thin layer of continuous PCL polymer (14,000 Da) film on CPT NRs using the solvent diffusion method.[29] Briefly, 1 ml each of 10 mg/ml of CPT in DMSO and 1 mg/ml of PCL polymer in toluene were added to a 20 ml of reverse osmosis (RO) water using a syringe pump. Residual toluene was removed by stirring (300 rpm) the CPT-PCL NR suspension overnight at room temperature (R.T.; ~22^{o}C). DMSO was removed by centrifugation at 3,000 rcf, followed by five times washing using RO water. PCL-coated CPT (CPT-PCL) NRs were freeze-dried, weighed and stored at 4^{o}C. CPT concentrations were measured, and quantified by reading absorbance at 366 nm using a plate reader (BioTek Synergy), and the CPT calibration curve.[18,29] The theoretical content of PCL weight in CPT-PCL NRs was calculated based on the weight of freeze-dried particles and CPT amount. Percent encapsulation efficiency of CPT and PCL were calculated based on their initial mass of samples.

2.2 CHARACTERIZATION OF CPT-PCL NRs

The morphology and size of CPT-PCL NRs were examined under transmission electron microscope (TEM; Tecnai F20) at an accelerating voltage of 120 kV. A drop of 10 µl CPT-PCL solutions in water was air-dried on carbon-coated copper grids (Tedpella). The NR diameter, NR length, and thickness of the polymer coating were measured using ImageJ (version 1.45S, NIH, USA). Uncoated CPT NRs were imaged using a scanning electron microscope (SEM; Helios Nanolab 600 FIB). The surface charges of NRs in PBS

were determined by dynamic light scattering using a NanoSeries Zetasizer ZS 90 (Malvern) and the backscattering detection at 90°. The zeta potential was measured for 15 runs. Data was analyzed using means and standard deviations of three concentrations.

2.3 DEGRADATION OF PCL COATING AND STABILITY OF LACTONE FORM OF CPT IN CPT-PCL NRS

The degradation of PCL coating, and conversion between lactone and carboxylates in CPT were analyzed by FT-IR spectroscopy. The disappearance of ester groups in PCL backbone, and appearance of carboxyl and hydroxyl groups were studied using FT-IR spectra. Briefly, CPT-PCL NRs were incubated for 72 h at 37°C in PBS at pH 6. Samples were freeze-dried to sublimate any water, and ground at 1:100 weight ratio with FT-IR grade potassium bromide (KBr; Alpha Aesar). Hydrolytic degradation was monitored by comparing the intensity of ester, alcohol and carboxyl bands at t=0 and 72 h for the same amount of PCL in NRs. To evaluate the conversion of active lactone rings into inactive carboxylic acids in coated NRs, CPT NRs alone without PCL coating was used as a control. The FT-IR absorbance spectra were obtained for 32 scans over the range of 4000 – 400 cm-1 using a Thermo Nicolet Nexus 470 FT-IR. Background noises were subtracted from the spectra. All spectra were analyzed using EZ OMNIC E.S.P v.5.1 software.

2.4 QUANTIFICATION OF CPT DRUG RELEASE

CPT drug release was conducted by exposing CPT-PCL NRs to phosphate buffered saline (PBS) at pH 6 (to mimic the cancer microenvironment) and pH 7.4, and at 37°C. PBS of 500 µl were sampled at different time intervals of t = 0, 0.5, 2, 4, 8, 24, 36 and 72 h. CPT drug concentrations, that were released to the buffer, were measured using absorbance at 366 nm and CPT standard curve. (These experiments were not run in

presence of fetal bovine serum (FBS) because FBS has high spectroscopic background noises).

2.5 CONJUGATION OF ANTIBODY ON THE SURFACE OF CPT-PCL NRs

TTZ antibody (Genentech) was conjugated to the surface of CPT-PCL NRs by coupling primary amines of TTZ with ester groups of PCL forming amide bonds. Briefly, 10 mg/ml TTZ solution was prepared in PBS of pH 7.4. 10 mg CPT-PCL NRs were added to 1 ml of TTZ solution, mixed, and incubated at R.T. The unreacted reagents were separated using 100 kDa membrane filters (EMD Millipore Amicon Ultra-0.5). The supernatants were collected by centrifugation at 1,000 rcf, and analyzed by the BCA protein assay (Pierce Thermo Scientific). Bovine serum albumin (BSA) was used to prepare HER-2 non-targeted CPT-PCL-BSA NRs.

2.6 *IN VITRO* CELL GROWTH INHIBITION

The effectiveness of combination treatments using CPT-PCL-TTZ NRs was evaluated in HER-2 positive BT-474 breast cancer cells (ATCC) and HER-2 negative cell line MDA-MB-231 (ATCC). The cells were cultured in Hybri-Care (ATCC), and RPMI 1640 (Life Technologies), respectively supplemented with 10% FBS (Corning) and 1% (100 units/ml) Penicillin-Streptomycin (Gibco) at 37^{o}C and 5% CO_2. Cells were plated in 96-well tissue culture plates (Corning) at a density of 10,000 cells/well in 200 µl respective medium. After 18 h of growth, 10 µl of NRs were added to the medium. The final concentrations of CPT were 0.1, 0.2, 0.5, 1, 2, 5 and 10 µg/ml. The corresponding PCL concentrations were 2.9 5.8, 14.6, 29.1, 58.2, 145.5 and 291.1 µg/ml, respectively, and TTZ concentrations were 0.4, 0.8, 1.9, 3.8, 7.5, 18.8 and 37.7 µg/ml, respectively. CPT-PCL-BSA was used as HER-2 non-specific control. Cells were also treated with the same

concentrations of PCL solutions to determine its cytotoxic effects. Cells treated with 10 µl of PBS were used as positive controls. 3 h later, the medium was replaced with fresh medium. After 72 h, the plates were centrifuged at 100 rcf for 15 min. The supernatant was discarded. Live cells were stained with 2 µM calcein AM (Life technologies) in PBS by incubating at R.T. for 30 min. The fluorescence intensity (F.I.) of calcein AM was measured using 485/528 excitation/emission filters using the plate reader (BioTek Synergy 2). The percentage inhibition in cell growth was calculated using the following equation (1):

$$\%\ inihibition\ in\ cell\ growth = \frac{F.I._{PBS\ treated\ cells} - F.I._{samples}}{F.I._{PBS\ treated\ cells}} \times 100 \qquad (1)$$

To examine that the cell growth inhibitory effects were induced by NRs intracellularly, BT-474 cells were incubated with CPT-PCL-TTZ NRs for 6 h at 37°C in 8-well glass chambers (Lab-Tek). TTZ was labeled with Alex Fluor 594 dye according to the manufacturer (Molecular Probes)'s protocol. After 2 h of NR incubation, the cells were washed with PBS three times to remove unbound particles, and re-incubated with medium for 4 h. Cells were imaged using a scanning laser inverted confocal microscope (Ti-Eclipse; Nikon) and 40x objective. The excitation/emission used for CPT and Alexa Fluor 594 were 360/400 and 590/617 nm, respectively.

2.7 STATISTICAL ANALYSIS

Each experiment was carried out with three independent experiments of at least triplicate measurements. The mean differences and standard deviations were evaluated.

3. RESULTS

3.1 PREPARATION OF A THIN LAYER OF PCL COATING ON CPT NRs

We developed an engineering technique based on the solvent diffusion method to prepare PCL coated CPT NRs of 500.9 ± 91.3 nm x 122.7 ± 10.1 nm in length and width, respectively (Fig. 3.1 (a)). This process involved 3-steps: phase separation, CPT NR

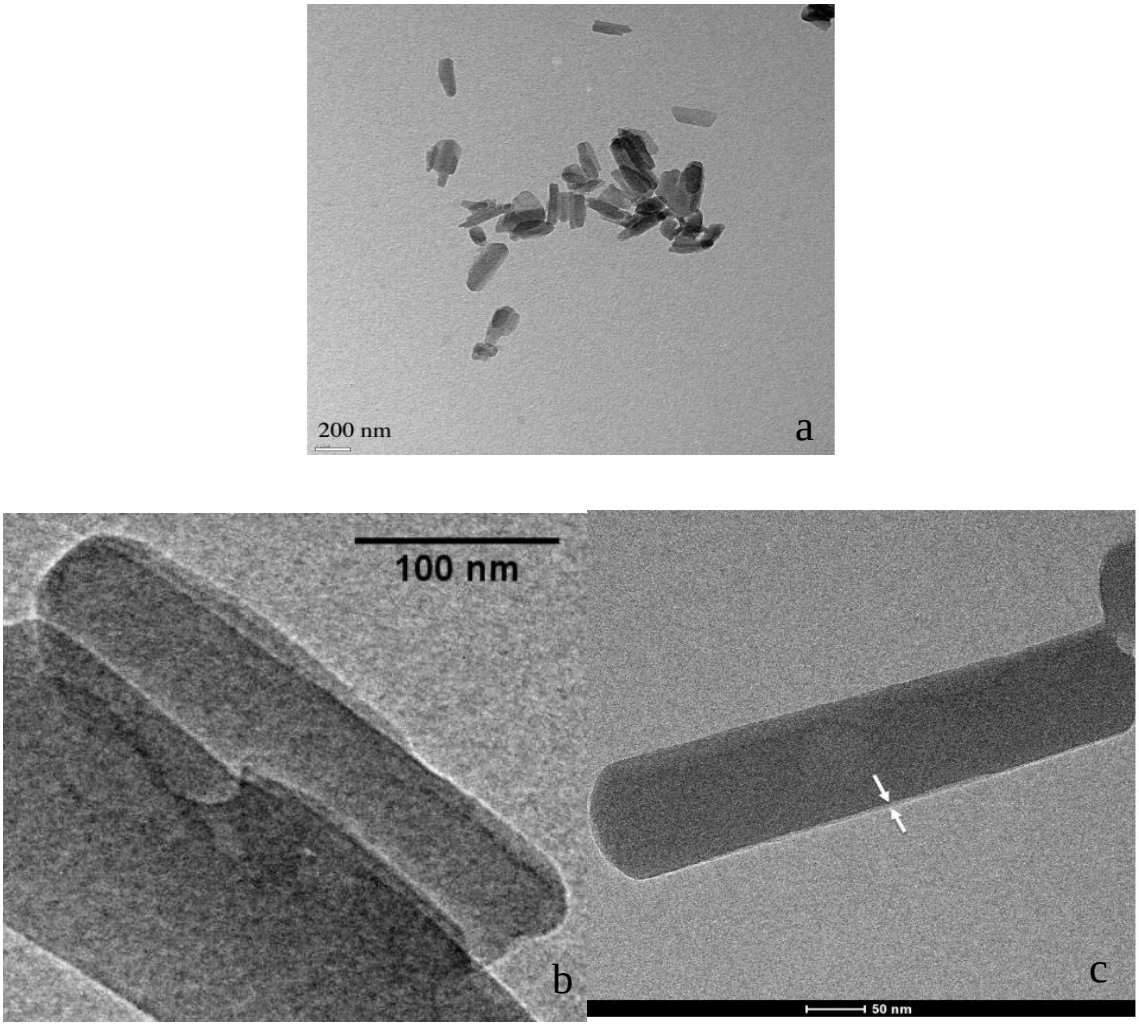

Figure 3.1: TEM images of CPT-PCL NRs. (a) Image showing homogeneous distribution of CPT-PCL NRs. (b) Magnified view of a thin (~10 nm; arrows) PCL polymer film on CPT NRs. (c) Polymer coating thickness

formation and PCL deposition. CPT NRs were formed because of phase separation from the DMSO oil phase into water under mild stirring (~300 rpm).[18,29] At the same time, continuous PCL polymer films were coated on CPT NRs by virtue of van der Waals attractive forces between CPT NR surface and PCL polymer under low shear stress.39 The combination of adhesive and shear forces spread the polymer thinly over CPT NRs. A thin layer of 10.3±1.4 nm PCL coating was formed surrounding the CPT NR (Fig. 3.1(b) and Fig 3.1(c)). This is a soft coating technique that does not require high mechanical agitation, sonication or vibration, thus preventing any structural damage of drugs. The encapsulation efficiency of drug: copolymers were reported 0.02 to 0.15.40 Zeta potentials of CPT NRs and CPT-PCL NRs were measured as -26.8 ± 7.71 mV (Fig. 3.2(a)) and -15.5 ± 3 mV (Fig. 3.2(b)) in PBS, respectively. An increase in zeta potential for CPT-PCL NRs indicates the deposition of the polymer on the surface of CPT NRs.

3.2 DEGRADATION OF PCL COATING USING FT-IR SPECTROSCOPY

The degradation of functional groups of PCL coating was determined by FT-IR analysis (Fig. 3.3). The infrared spectra of CPT-PCL NRs were compared before (t=0; Fig. 3.3, top, dotted line) and after (t=72 h; Fig. 3.3, middle, solid line) incubation in PBS at pH 6 that mimics the slightly acidic cancer microenvironment. The presence of strong band at 1746 cm^{-1} is due to the presence of ester carbonyl group that corresponds to the –CO stretching in PCL polymer coating before degradation (dotted line). The band intensity at 1746 cm^{-1} decreased after 72 h due to hydrolytic cleavage of ester bonds at pH 6 (solid line). The peak at 1288 cm^{-1} represents C-C and C=O stretching in the PCL polymer backbone,[41] which decreases in intensity at t=72 h. The peaks at 2860 and 2930 cm^{-1} correspond to the characteristic absorption of the C-H stretching bonds of ε-CL. The

appearance of two peaks at 1460 and 2370 cm^{-1} in t=72 h spectra are characteristics of -OH functional group in carboxylic acid (-COOH) indicating the hydrolysis of ester bonds.

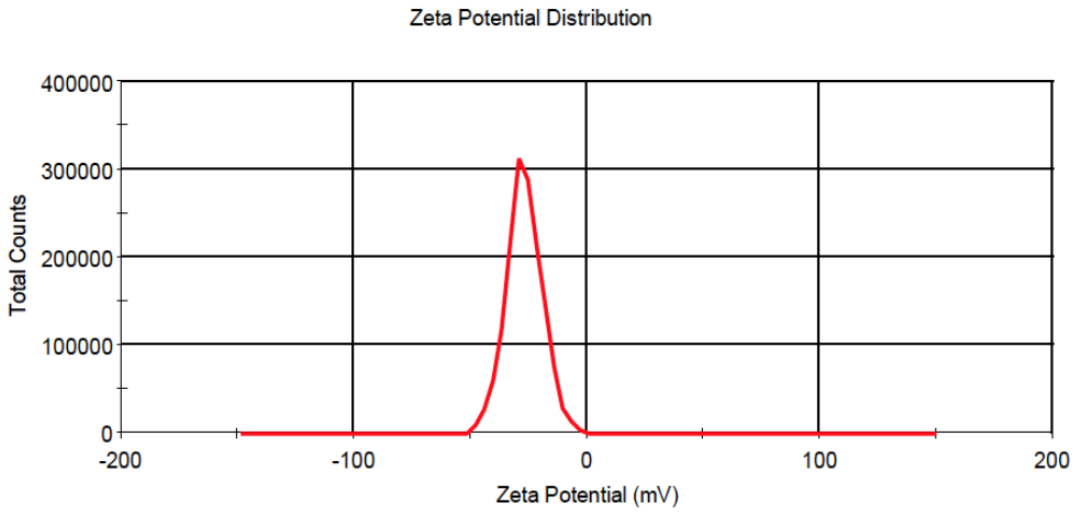

a

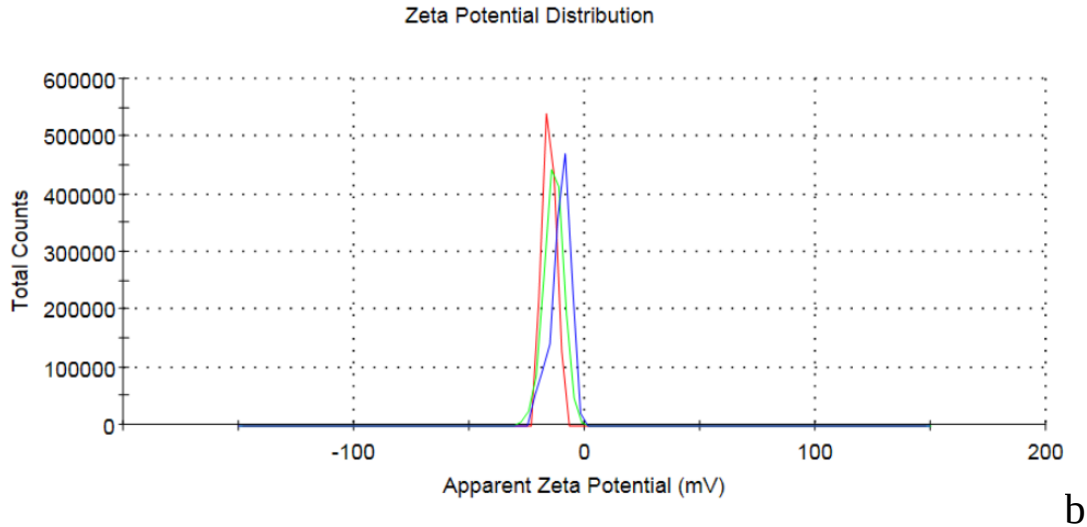

b

Figure 3.2: Surface zeta potential of CPT NRs (a) before PCL coating, and (b) after PCL coating as analyzed using DLS. Three colored lines indicate three replicates with a symmetric distribution of zeta potential.

OH functional group in carboxylic acid (-COOH) indicating the hydrolysis of ester bonds. The peak at 3420 cm^{-1} indicates the presence of H-O-H stretching in water that increases in intensity slightly at t=72 h. The absorption band of hydroxyl group is also present at t=0 h with a slightly shorter peak, which, may be, due to absorption of moisture from the

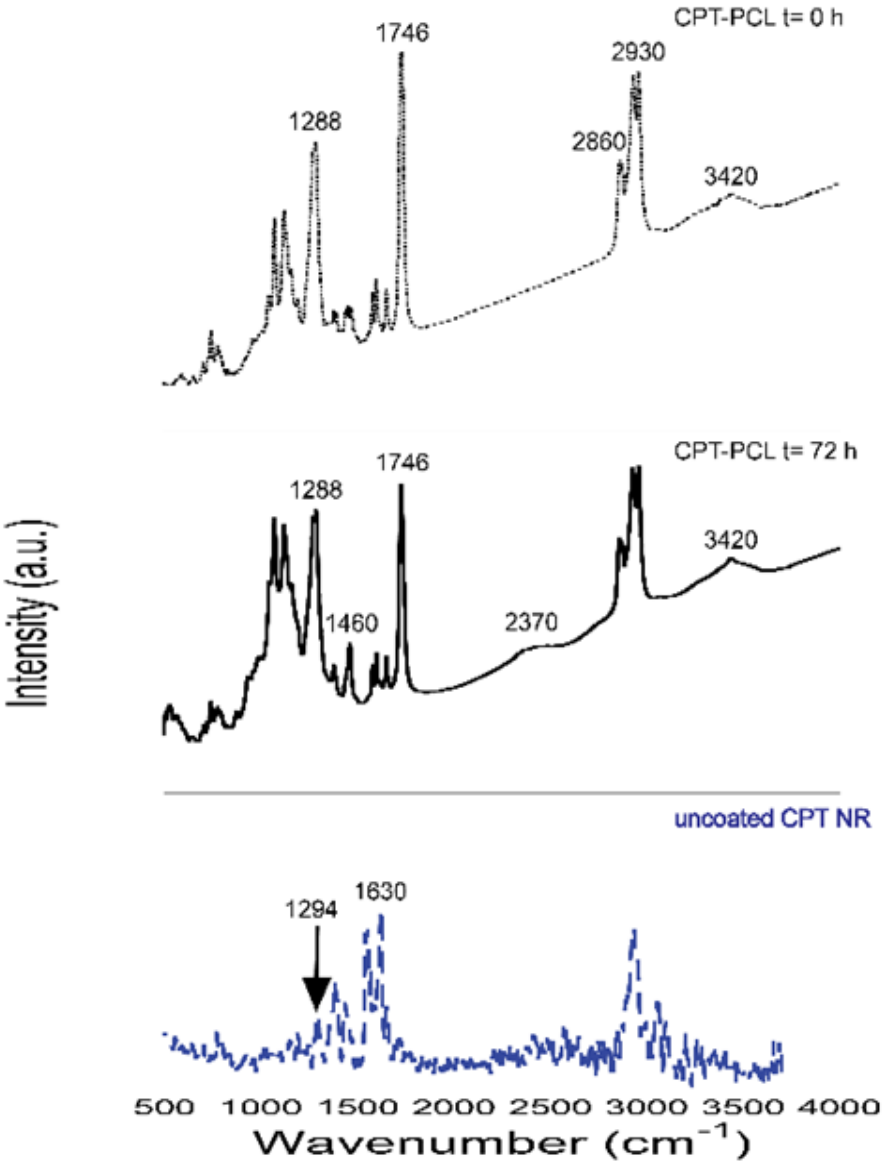

Figure 3.3: FT-IR graphs of CPT-PCL NRs at t=0 (dotted line), t=72 h (solid line) and CPT NRs without any coating

atmosphere. The FT-IR spectra of CPT NRs without PCL coating (Fig. 3.3, bottom, dash line) shows carbonyl stretching for cyclic ester (lactone) at 1630 cm^{-1} and C-C(=O)-O stretching for carboxylate at 1294 cm^{-1}.[42] We calculated the ratio of intensity peaks of lactone: carboxylate that was 2.81 in uncoated CPT NRs. This ratio of lactone: carboxylate decreased to only 0.8 in CPT-PCL NRs suggesting the protection of an active form of lactone rings underlying the PCL coating.

3.3 CPT DRUG RELEASE WITH PCL COATING DEGRADATION

The percentage of CPT release at different time intervals is shown in Fig. 3.4 as calculated using the CPT standard curve (Fig. 3.5). A slow release was observed at pH 6

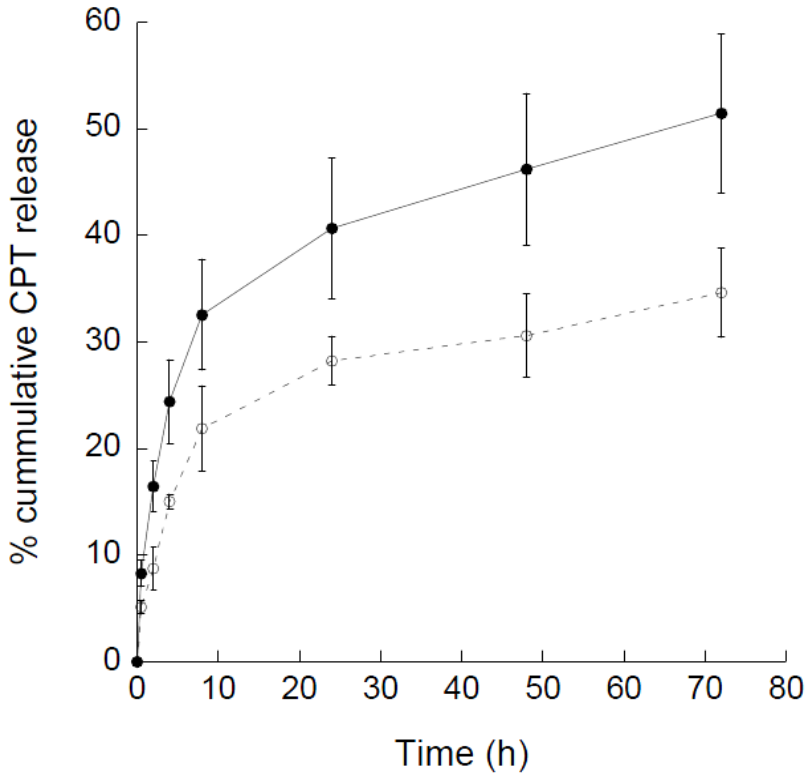

Figure 3.4: Cumulative percentage of CPT drug release from CPT-PCL NRs in PBS buffer at pH 6 (solid line, solid points) and pH 7.4 (dotted line, open points), and at 37°C *versus* time

(solid line) with 8.2% CPT release in the first 0.5 h following 32.6% release after 8 h, and 51.5% after 72 h. The release rate is comparable with the release patterns of CPT from poly(D,L-lactide-co-glycolic acid) (PLGA) microspheres,[43] and HCPT-1 from PCLLA-

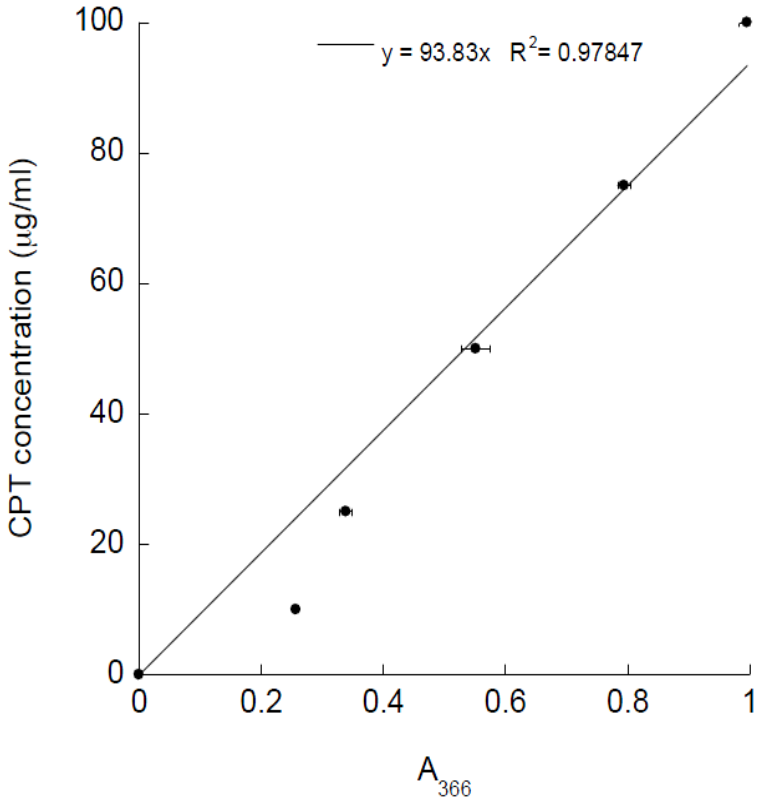

Figure 3.5: The CPT standard curve was used to measure the drug concentrations

PEG-PCLLA.33 At pH 7.4 (dotted line), the release profile was slower, and it needs almost 72 h to reach ~30% release, indicating the coating effect of bioresponsive PCL barrier. CPT was released from PCL-coated NRs at pH 6 by hydrolytic disruption of PCL coating and the drug's diffusion.

3.4 PREPARATION OF ANTIBODY TARGETED CPT-PCL-TTZ NRs

TTZ antibody was conjugated on the surface of CPT-PCL NRs by amide bond formation between the ester groups of polymer and amines on the antibody. The advantage

of this method is the avoidance of preliminary modifications of the antibody such as activation by carbodiimide that reduces its activity.[46] TTZ covalent binding will help to deliver the NRs at breast cancer cells. The encapsulation efficiency was expressed as the weight ratio among CPT, PCL and proteins (TTZ or BSA) incorporated in NRs (Table 3.1). The protein concentrations were measured using the BCA protein assay and BSA standard curve (Fig. 3.6). The weight ratio of CPT: PCL: TTZ and CPT: PCL: BSA were calculated as 12: 1: 9 and 13.9: 1: 9.4, respectively (Table 3.1). Table 3.2 shows the percentage encapsulation of CPT, PCL, TTZ and BSA in respective NRs.

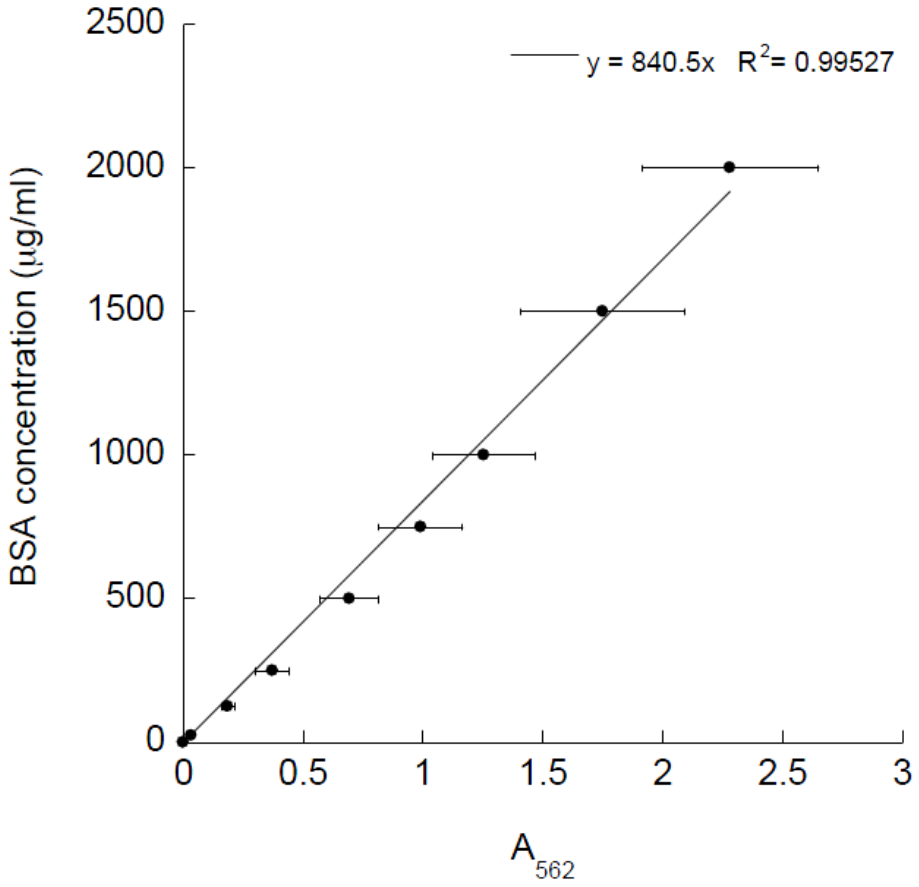

Figure 3.6: The BSA standard curve was used to measure protein concentrations.

Table 3.1: Characterization of CPT-PCL-TTZ and CPT-PCL-BSA NR conjugates

CPT in CPT-PCL-TTZ NRs, mg	4.8 ± 1.3
PCL in CPT-PCL-TTZ NRs, mg	0.4 ± 0.05
TTZ in CPT-PCL-TTZ NRs, mg	3.7 ± 1.6
CPT: PCL: TTZ (w: w ratio)	12 : 1 : 9
CPT in CPT-PCL-BSA NRs, mg	5 ± 0.8
PCL in CPT-PCL-BSA NRs, mg	0.36 ± 0.9
BSA in CPT-PCL-BSA NRs. mg	3.4 ± 1.7
CPT: PCL: BSA (w: w ratio)	13.9 : 1 : 9.4

Table 3.2: Encapsulation efficiency for CPT, PCL, TTZ and BSA in NR forms

Component	**% encapsulation/ conjugation efficiency**
CPT	49.2 ± 1.1
PCL	39.9 ± 5.9
TTZ	41.1 ± 1.8
BSA	33.7 ± 1.8

3.5 INHIBITION OF BREAST CANCER CELL GROWTH BY CPT-PCL-TTZ NRs

The therapeutic activity of CPT-PCL-TTZ NRs was evaluated in HER-2 positive BT-474 (Fig. 3.7) and HER-2 negative MDA-MB-231 cells (Fig. 3.8) at varying concentrations. These are the previously reported doses of CPT in human breast cancer cells.[7,8,29,47] The NRs inhibited the growth of HER-2 positive BT-474 cells in a dose

dependent manner. The combination of CPT and TTZ using CPT-PCL-TTZ NRs inhibited up to 61.6% BT-474 cell growth at 10 µg/ml. At this concentration, CPT-PCL-TTZ NRs inhibited the cell growth 1.5 fold more than CPT-PCL-BSA NRs. The difference in growth inhibition between CPT-PCL-TTZ and CPT-PCL-BSA indicates the antibody dependent growth inhibition effects of TTZ on HER-2 positive BT-474 cells.[48,49] Surprisingly HER-2 negative MDA-MB-231 cell line was also sensitive to the NRs (Fig. 3.8). No difference between CPT-PCL-BSA and CPT-PCL-TTZ was found in these cells, indicating non-specific CPT-evoked growth inhibition.

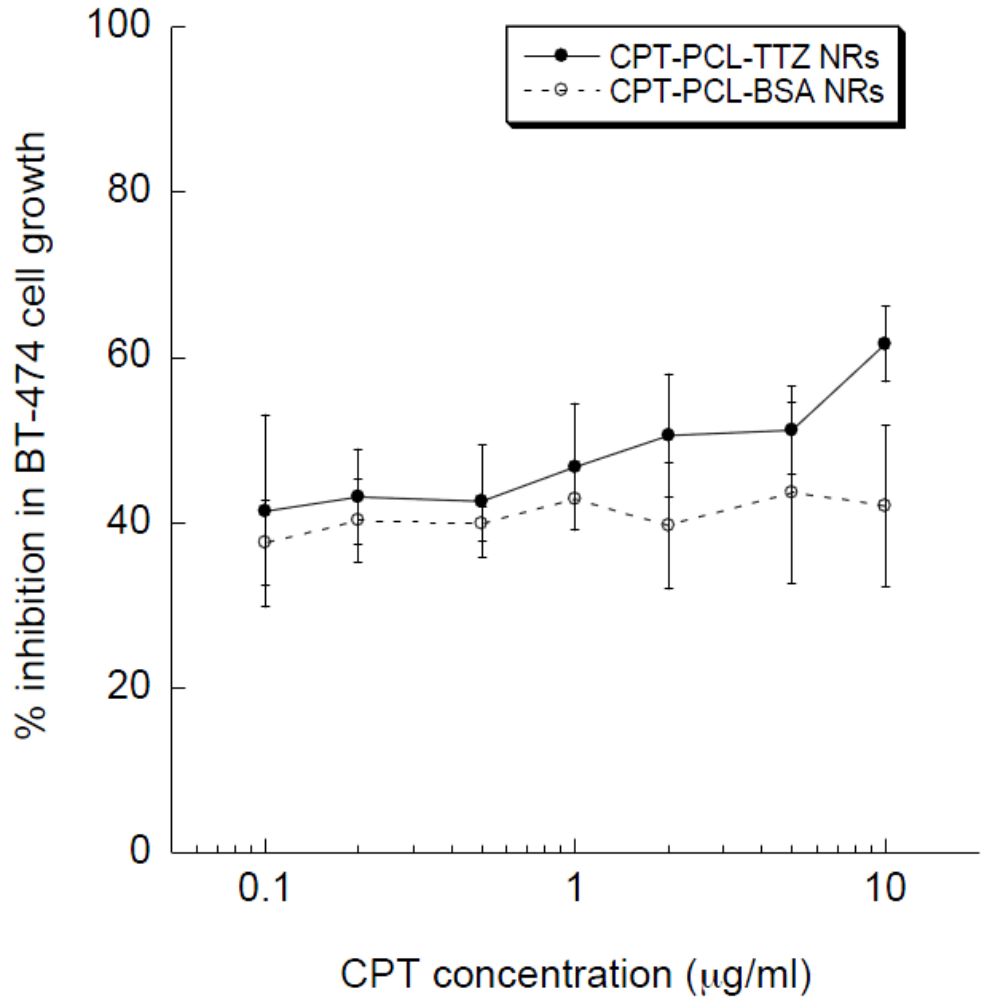

Figure 3.7: Growth inhibition curves of HER-2 positive BT-474 cells as determined by calcein-AM live dead assay after 72 h incubation. Results are expressed as a percentage of PBS-treated control cells *versus* doses of CPT in CPT-PCL-TTZ NRs. The data represent average and standard deviation of ten treatments in three independent experiments.

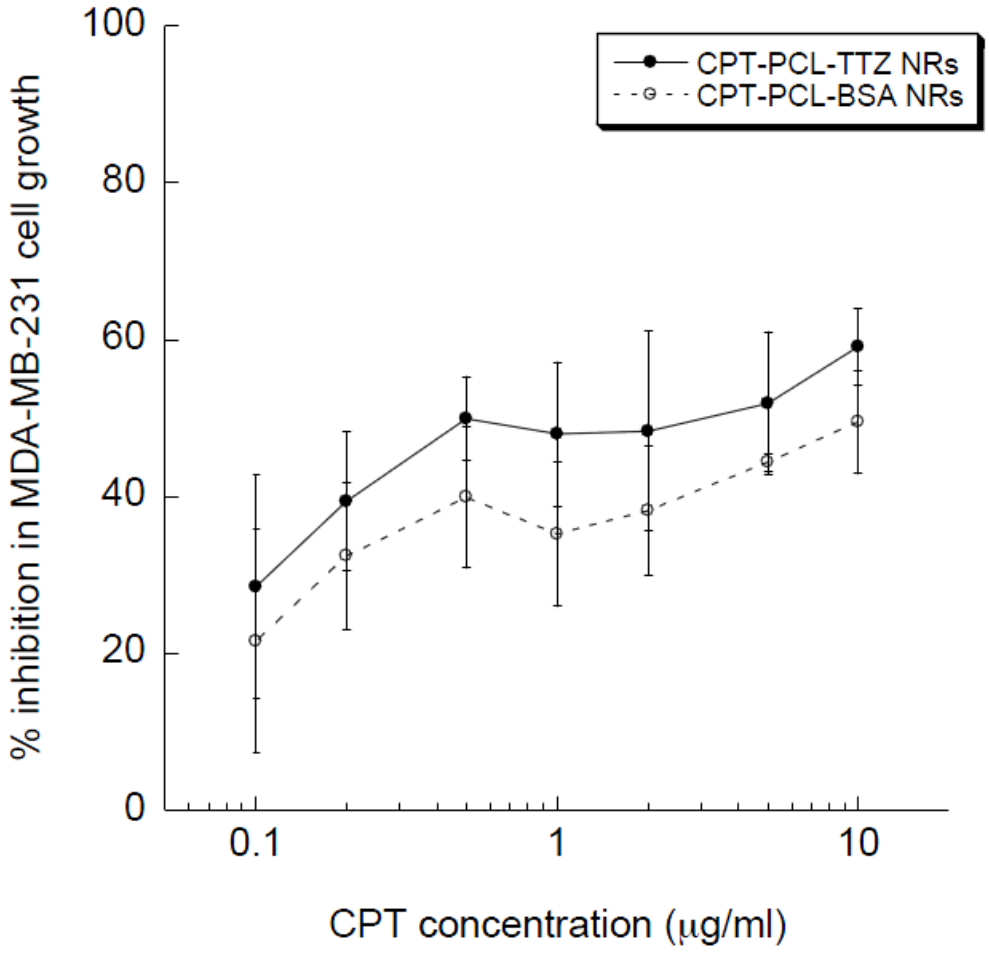

Figure 3.8: Growth inhibitory effects of CPT-PCL-TTZ NRs on HER-2 negative MDA-MB-231 cells. No difference between CPT-PCL-TTZ and CPT-PCL-BSA control indicates non-targeted CPT mediated cytotoxicity only in MDA-MB-231 cell

4. DISCUSSION

Our proposed polymer-coated drug NRs have advantages over uncoated drugs in that they can avoid rapid body clearance, have fewer side effects in normal healthy cells, and can protect drugs from premature degradation. At physiological pH, the unstable E-ring lactone in CPT is converted to carboxylate form, which possesses high affinity to human serum albumin (HSA) and is preferentially eliminated.[1,2] This is a clinical hurdle to CPT therapeutic efficiency. Encapsulation of CPT inside PCL polymer coating prevents CPT from being converted into the inactive carboxylate form during blood circulation, thus increasing its likelihood of reaching the tumor intact.[50,51] As it is observed from the FT-IR data (Fig. 3.3) that the PCL coating undergoes hydrolytic degradation producing non-toxic by-products (alcohol and water). Slow degradation of the polymers released CPT drugs from NRs at pH 6 (Fig. 3.4; solid line). At pH 7.4, PCL polymer coating does not allow for fast CPT penetration (Fig. 3.4; dotted line).

The elongated NR design allows for long circulation time in the body,[24,26,52-54] and multivalent interactions with tumor cells,[21,55,56] increasing the probability of receptor-ligand interactions. It is shown that the active targeting of breast cancer cells using the similar dimension of NRs of CPT with TTZ attached to the breast cancer cell surface.[18,29] Due to the fluid dynamics induced by the unique rod shape, these nanoparticles flow along the edges of blood vessels. By flowing along the sides of blood vessels, nanoparticles fall to the tumor due to gaps in the endothelial cell wall between the tumorous tissue and blood vessels.[57] The layer of TTZ antibody on the surface of NRs offers additional feature of targeted therapy.

The tumor microenvironment is slightly more acidic (pH ~6) than the blood (pH 7.4).[58,59] We simulated the condition using PBS at pH 6 and determined the effects on the stability of NRs. The release of CPT in the first 30 minutes was minimal, with only 7.4% of the total CPT drugs in NRs being released (Fig. 3.4; solid line). The polymer coating begins to disintegrate, releasing ~40% of total CPT in 24 h and more than 50.8% in 72 h.

Interaction with cancer cells is important for most nanoparticles reaching the target site. By changing nanoparticle geometry from spherical to rod-shape, receptor-ligand interactions can be enhanced up to 2.5 fold by multivalency effects.[18] We accomplished active targeting by conjugating TTZ to the surface of CPT-PCL NRs. By using both CPT and TTZ, which use different mechanisms of actions of cytotoxicity, we find increased therapeutic efficacy over those of traditional monotherapies. CPT is a topoisomerase I (topoI) inhibitor that selectively affects cancer cells by exerting S-phase cytotoxicity and G2-M cell cycle arrest.[1,2] TTZ induces cell cycle arrest in the G1 phase leading to apoptosis.[37,38] While CPT is cytotoxic and the single agent therapeutic response rate of TTZ is low (~26%),[6,33,37,48,49,60-62] the combination approach is more effective in treating cancers than monotherapies, as the probability of acquiring resistance to two simultaneous treatments is the square of the probability of resistance to a single agent.

We observed that HER-2 negative MDA-MB-231 cell line was sensitive to NRs (Fig. 3.8). No difference between CPT-PCL-BSA and CPT-PCL-TTZ was found in these cells. We conjecture that this might be due to effective non-specific endocytosis in *in vitro* setting. We anticipate difference in targeting efficiency shall be observed in *in vivo* setting. Collectively, our results support a purely cytostatic effect of these drugs *in vitro*, we are

currently at the stage of performing in vivo experiments to examine this combination in mice xenograft models.

5. CONCLUSIONS

We have developed a simple method of thin (10.3±1.4 nm) layer of bioresponsive PCL polymer coating on CPT anti-cancer drug NRs. As the drug molecules precipitated out of its organic solvent into an aqueous phase, the molecules aggregated and formed NRs. The PCL polymers spread thinly over drug NRs due to van der Waals and hydrogen bonding effects. This process did not produce any adverse mechanical effects to prepare the NRs, thereby, retaining active structures of therapeutic drugs. One merit of our method is the preparation of PCL-coated CPT NRs of (500.9±91.3 x 122.7±10.1) nm size in large quantities. We characterized the degradation of CPT-PCL NRs using FT-IR analysis, and release of CPT in a simulated pH condition in caner microenvironment. Conjugation of TTZ to the surface of CPT-PCL NRs significantly inhibited the growth of BT-474 breast cancer cells. Overexpression of HER-2 increases breast cancer cell proliferation in part by transactivation of enhanced growth factor receptor (EGFR) signaling.[37,48,61] Blocking of HER-2 by selective TTZ binding proved to suppress the cells growth. In vivo studies are needed for therapeutic efficacy. Nonetheless, our current results found thus far are promising and continue to shed light of the inherent benefits of improved breast cancer therapy

6. ACKNOWLEDGMENTS

The authors would like to thank Dr. Jessica Terbush for TEM images. We would like to acknowledge the Environmental Research Center (ERC) and Materials Research Center (MRC) at Missouri S & T for TEM and Zetasizer use. This research was funded by S.B.'s start-up and the Center for Biomedical Science and Engineering (CBSE) seed funding. T.L. was supported by a fellowship from the Government of Thailand. K.D. and C.B. were supported by OURE fellowships at Missouri S & T.

REFERENCES

1. Jaxel, C.; Capranico, G.; Kerrigan, D.; Kohn, K. W.; Pommier, Y., Effect of local DNA sequence on topoisomerase I cleavage in the presence or absence of camptothecin. *Journal of Biological Chemistry* **1991**, 266, 20418-23.

2. Jaxel, C.; Kohn, K. W.; Wani, M. C.; Wall, M. E.; Pommier, Y., Structure-Activity Study of the Actions of Camptothecin Derivatives on Mammalian Topoisomerase I: Evidence for a Specific Receptor Site and a Relation to Antitumor Activity. *Cancer Research* **1989**, 49, 1465-1469.

3. Svenson, S.; Wolfgang, M.; Hwang, J.; Ryan, J.; Eliasof, S., Preclinical to clinical development of the novel camptothecin nanopharmaceutical CRLX101. *Journal of Controlled Release* **2011**, 153, 49-55.

4. Homsi, J.; Simon, G. R.; Garrett, C. R.; Springett, G.; De Conti, R.; Chiappori, A. A.; Munster, P. N.; Burton, M. K.; Stromatt, S.; Allievi, C.; Angiuli, P.; Eisenfeld, A.; Sullivan, D. M.; Daud, A. I., Phase I Trial of Poly-l-Glutamate Camptothecin (CT-2106) Administered Weekly in Patients with Advanced Solid Malignancies. *Clinical Cancer Research* **2007**, 13, 5855-5861.

5. Han, H.; Davis, M. E., Single-Antibody, Targeted Nanoparticle Delivery of Camptothecin. *Molecular pharmaceutics* **2013**, 10, 2558-2567.

6. Schluep, T.; Hwang, J.; Cheng, J.; Heidel, J. D.; Bartlett, D. W.; Hollister, B.; Davis, M. E., Preclinical Efficacy of the Camptothecin-Polymer Conjugate IT-101 in Multiple Cancer Models. *Clinical Cancer Research* **2006**, 12, 1606-1614.

7. Cheng, J.; Khin, K. T.; Jensen, G. S.; Liu, A.; Davis, M. E., Synthesis of Linear, β-Cyclodextrin-Based Polymers and Their Camptothecin Conjugates. *Bioconjugate Chemistry* **2003**, 14, 1007-1017.

8. Cheng, J.; Khin, K. T.; Davis, M. E., Antitumor activity of beta-cyclodextrin polymer-camptothecin conjugates. *Mol Pharm* **2004**, 1, 183-193.

9. Bissett, D.; Cassidy, J.; De Bono, J. S.; Muirhead, F.; Main, H.; Robson, L.; Fraier, D.; Magnè, M. L.; Pellizzoni, C.; Porro, M. G.; Spinelli, R.; Speed, W.; Twelves, C., Phase I and pharmacokinetic (PK) study of MAG-CPT (PNU 166148): A polymeric derivative of camptothecin (CPT). *British Journal of Cancer* **2004**, 91, 50-55.

10. Oledzka, E.; Horeglad, P.; Gruszczyńska, Z.; Plichta, A.; Nałęcz-Jawecki, G.; Sobczak, M., Polylactide Conjugates of Camptothecin with Different Drug Release Abilities. *Molecules* **2014**, 19, 19460.

11. Chen, X.; McRae, S.; Parelkar, S.; Emrick, T., Polymeric Phosphorylcholine−Camptothecin Conjugates Prepared by Controlled Free Radical Polymerization and Click Chemistry. *Bioconjugate Chemistry* **2009**, 20, 2331-2341.

12. Batist, G.; Gelmon, K. A.; Chi, K. N.; Miller, W. H.; Chia, S. K. L.; Mayer, L. D.; Swenson, C. E.; Janoff, A. S.; Louie, A. C., Safety, Pharmacokinetics, and Efficacy of CPX-1 Liposome Injection in Patients with Advanced Solid Tumors. *Clinical Cancer Research* **2009**, 15, 692-700.

13. Yanagihara, K.; Takigahira, M.; Kubo, T.; Ochiya, T.; Hamaguchi, T.; Matsumura, Y., Marked antitumor effect of NK012, a SN-38-incorporating micelle formulation, in a newly developed mouse model of liver metastasis resulting from gastric cancer. *Therapeutic Delivery* **2014**, 5, 129-138.

14. Bissett, D.; Cassidy, J.; de Bono, J. S.; Muirhead, F.; Main, M.; Robson, L.; Fraier, D.; Magnè, M. L.; Pellizzoni, C.; Porro, M. G.; Spinelli, R.; Speed, W.; Twelves, C., Phase I and pharmacokinetic (PK) study of MAG-CPT (PNU 166148): a polymeric derivative of camptothecin (CPT). *British Journal of Cancer* **2004**, 91, 50-55.

15. Yurkovetskiy, A. V.; Fram, R. J., XMT-1001, a novel polymeric camptothecin pro-drug in clinical development for patients with advanced cancer. *Advanced Drug Delivery Reviews 2009*, 61, 1193-1202.

16. Coelho, J. F.; Ferreira, P. C.; Alves, P.; Cordeiro, R.; Fonseca, A. C.; Góis, J. R.; Gil, M. H., Drug delivery systems: Advanced technologies potentially applicable in personalized treatments. *The EPMA Journal* **2010**, 1, 164-209.

17. Yan, G.; Paul, D.; Shenshen, C.; Richard, T.; Manorama, T.; Tamara, M.; Dennis, E. D., Shape effects of filaments versus spherical particles in flow and drug delivery. *Nature Nanotechnology* **2007**, 2, 249-255.

18. Barua, S.; Yoo, J.-W.; Kolhar, P.; Wakankar, A.; Gokarn, Y. R.; Mitragotri, S., Particle shape enhances specificity of antibody-displaying nanoparticles. *Proceedings of the National Academy of Sciences* **2013**, 110, 3270-3275.

19. Decuzzi, P.; Ferrari, M., The adhesive strength of non-spherical particles mediated by specific interactions. *Biomaterials* **2006**, 27, 5307-5314.

20. Decuzzi, P.; Ferrari, M., The Receptor-Mediated Endocytosis of Nonspherical Particles. *Biophysical Journal* **2008**, 94, 3790-3797.

21. Gratton, S. E. A.; Ropp, P. A.; Pohlhaus, P. D.; Luft, J. C.; Madden, V. J.; Napier, M. E.; DeSimone, J. M., The effect of particle design on cellular internalization pathways. *Proceedings of the National Academy of Sciences* **2008**, 105, 11613-11618.

22. Huang, X.; Teng, X.; Chen, D.; Tang, F.; He, J., The effect of the shape of mesoporous silica nanoparticles on cellular uptake and cell function. *Biomaterials* **2010**, 31, 438-448.

23. Champion, J. A.; Mitragotri, S., Role of target geometry in phagocytosis. *Proceedings of the National Academy of Sciences of the United States of America* **2006**, 103, 4930-4.

24. Muro, S.; Garnacho, C.; Champion, J. A.; Leferovich, J.; Gajewski, C.; Schuchman, E. H.; Mitragotri, S.; Muzykantov, V. R., Control of Endothelial Targeting and Intracellular Delivery of Therapeutic Enzymes by Modulating the Size and Shape of ICAM-1-targeted Carriers. Molecular therapy : *the journal of the American Society of Gene Therapy* **2008**, 16, 1450-1458.

25. Gentile, F.; Chiappini, C.; Fine, D.; Bhavane, R. C.; Peluccio, M. S.; Cheng, M. M.-C.; Liu, X.; Ferrari, M.; Decuzzi, P., The effect of shape on the margination dynamics of non-neutrally buoyant particles in two-dimensional shear flows. *Journal of Biomechanics* **2008**, 41, 2312-2318.

26. Decuzzi, P.; Godin, B.; Tanaka, T.; Lee, S. Y.; Chiappini, C.; Liu, X.; Ferrari, M., Size and shape effects in the biodistribution of intravascularly injected particles. *Journal of Controlled Release* **2010**, 141, 320-327.

27. Adriani, G.; de Tullio, M. D.; Ferrari, M.; Hussain, F.; Pascazio, G.; Liu, X.; Decuzzi, P., The preferential targeting of the diseased microvasculature by disk-like particles. *Biomaterials* **2012**, 33, 5504-5513.

28. Godin, B.; Chiappini, C.; Srinivasan, S.; Alexander, J. F.; Yokoi, K.; Ferrari, M.; Decuzzi, P.; Liu, X., Drug Delivery: Discoidal Porous Silicon Particles: Fabrication and Biodistribution in Breast Cancer Bearing Mice (Adv. Funct. Mater. 20/2012). *Advanced Functional Materials* **2012**, 22, 4186-4186.

29. Barua, S.; Mitragotri, S., Synergistic Targeting of Cell Membrane, Cytoplasm, and Nucleus of Cancer Cells Using Rod-Shaped Nanoparticles. *ACS Nano* **2013**, 7, 9558-9570.

30. Woodruff, M. A.; Hutmacher, D. W., The return of a forgotten polymer—Polycaprolactone in the 21st century. *Progress in Polymer Science* **2010**, 35, 1217-1256.

31. Kumari, A.; Yadav, S. K.; Yadav, S. C., Biodegradable polymeric nanoparticles based drug delivery systems. Colloids and Surfaces B: *Biointerfaces* **2010**, 75, 1-18.

32. Yang, Y.-Y.; Chung, T.-S.; Ping Ng, N., Morphology, drug distribution, and in vitro release profiles of biodegradable polymeric microspheres containing protein fabricated by double-emulsion solvent extraction/evaporation method. *Biomaterials* **2001**, 22, 231-241.

33. Zhang, L.; Yang, M.; Wang, Q.; Li, Y.; Guo, R.; Jiang, X.; Yang, C.; Liu, B., 10-Hydroxycamptothecin loaded nanoparticles: Preparation and antitumor activity in mice. *Journal of Controlled Release* **2007**, 119, 153-162.

34. Kang, Y. M.; Kim, G. H.; Kim, J. I.; Kim, D. Y.; Lee, B. N.; Yoon, S. M.; Kim, J. H.; Kim, M. S., In vivo efficacy of an intratumorally injected in situ-forming doxorubicin/poly(ethylene glycol)-b-polycaprolactone diblock copolymer. *Biomaterials* **2011**, 32, 4556-4564.

35. Gao, H.; Wang, Y. N.; Fan, Y. G.; Ma, J. B., Synthesis of a biodegradable tadpole-shaped polymer via the coupling reaction of polylactide onto mono(6-(2-aminoethyl)amino-6-deoxy)-β- cyclodextrin and its properties as the new carrier of protein delivery system. *Journal of Controlled Release* **2005**, 107, 158-173.

36. Barua, S.; Yoo, J. W.; Kolhar, P.; Wakankar, A.; Gokarn, Y. R.; Mitragotri, S., Particle shape enhances specificity of antibody-displaying nanoparticles. *Proceedings of the National Academy of Sciences of the United States of America* **2013**, 110, 3270-3275.

37. Boekhout, A. H.; Beijnen, J. H.; Schellens, J. H. M., Trastuzumab. *The Oncologist* **2011**, 16, 800-810.

38. Dean-Colomb, W.; Esteva, F. J., Her2-positive breast cancer: Herceptin and beyond. *European Journal of Cancer* **2008**, 44, 2806-2812.

39. Chen, E.-C.; Wu, T.-M., Isothermal crystallization kinetics and thermal behavior of poly(ε-caprolactone)/multi-walled carbon nanotube composites. *Polymer Degradation and Stability* **2007**, 92, 1009-1015.

40. Zhang, L.; Hu, Y.; Jiang, X.; Yang, C.; Lu, W.; Yang, Y. H., Camptothecin derivative-loaded poly(caprolactone-co-lactide)-b-PEG-b-poly(caprolactone-co-lactide) nanoparticles and their biodistribution in mice. *Journal of Controlled Release* **2004**, 96, 135-148.

41. Elzein, T.; Nasser-Eddine, M.; Delaite, C.; Bistac, S.; Dumas, P., FTIR study of polycaprolactone chain organization at interfaces. *Journal of Colloid and Interface Science* **2004**, 273, 381-387.

42. Tong, W.; Wang, L.; D'Souza, M. J., Evaluation of PLGA Microspheres as Delivery System for Antitumor Agent-Camptothecin. *Drug Development and Industrial Pharmacy* **2003**, 29, 745-756.

43. Ertl, B.; Platzer, P.; Wirth, M.; Gabor, F., Poly(D,L-lactic-co-glycolic acid) microspheres for sustained delivery and stabilization of camptothecin. *Journal of Controlled Release* **1999**, 61, 305-317.

44. Korsmeyer, R. W.; Gurny, R.; Doelker, E.; Buri, P.; Peppas, N. A., Mechanisms of solute release from porous hydrophilic polymers. *International Journal of Pharmaceutics* **1983**, 15, 25-35.

45. Peppas, N. A., Analysis of Fickian and non-Fickian drug release from polymers. *Pharmaceutica Acta Helvetiae* **1985**, 60, 110-111.

46. Kocbek, P.; Obermajer, N.; Cegnar, M.; Kos, J.; Kristl, J., Targeting cancer cells using PLGA nanoparticles surface modified with monoclonal antibody. *Journal of Controlled Release* **2007**, 120, 18-26.

47. Cirpanli, Y.; Bilensoy, E.; Dogan, A. L.; Calis, S., Development of polymeric and cyclodextrin nanoparticles for camptothecin delivery. *Journal of Controlled Release* **2010**, 148, e21-e23.

48. Sadeghi, S.; Olevsky, O.; Hurvitz, S. A., Profiling and targeting HER2-positive breast cancer using trastuzumab emtansine. *Pharmacogenomics & Personalized Medicine* **2014**, 7, 329-338.

49. Lewis Phillips, G. D.; Li, G.; Dugger, D. L.; Crocker, L. M.; Parsons, K. L.; Mai, E.; Blättler, W. A.; Lambert, J. M.; Chari, R. V. J.; Lutz, R. J.; Wong, W. L. T.; Jacobson, F. S.; Koeppen, H.; Schwall, R. H.; Kenkare-Mitra, S. R.; Spencer, S. D.; Sliwkowski, M. X., Targeting HER2-Positive Breast Cancer with Trastuzumab-DM1, an Antibody–Cytotoxic Drug Conjugate. *Cancer Research* **2008**, 68, 9280-9290.

50. Huang, Y.-Y.; Chung, T.-W.; Tzeng, T.-W., A method using biodegradable polylactides/polyethylene glycol for drug release with reduced initial burst. *International Journal of Pharmaceutics* **1999**, 182, 93-100.

51. Xue, M.; Hu, H.; Jiang, Y.; Liu, J.; He, H.; Ye, X., Biodegradable Polymer-Coated, Gelatin Hydrogel/Bioceramics Ternary Composites for Antitubercular Drug Delivery and Tissue Regeneration. *Journal of Nanomaterials* **2012**, 2012, 8.

52. Geng, Y.; Dalhaimer, P.; Cai, S.; Tsai, R.; Tewari, M.; Minko, T.; Discher, D. E., Shape effects of filaments versus spherical particles in flow and drug delivery. *Nat Nano* **2007**, 2, 249-255.

53. Kolhar, P.; Anselmo, A. C.; Gupta, V.; Pant, K.; Prabhakarpandian, B.; Ruoslahti, E.; Mitragotri, S., Using shape effects to target antibody-coated nanoparticles to lung and brain endothelium. *Proceedings of the National Academy of Sciences* **2013**, 110, 10753-10758.

54. Liu, Y.; Tan, J.; Thomas, A.; Ou-Yang, D.; Muzykantov, V. R., The shape of things to come: importance of design in nanotechnology for drug delivery. *Therapeutic delivery* **2012**, 3, 181-194.

55. Perry, J. L.; Herlihy, K. P.; Napier, M. E.; DeSimone, J. M.: PRINT, A Novel Platform Toward Shape and Size Specific Nanoparticle Theranostics. *Accounts of Chemical Research* **2011**, 44, 990-998.

56. Fromen, C. A.; Robbins, G. R.; Shen, T. W.; Kai, M. P.; Ting, J. P. Y.; DeSimone, J. M., Controlled analysis of nanoparticle charge on mucosal and systemic antibody responses following pulmonary immunization. *Proceedings of the National Academy of Sciences* **2015**, 112, 488-493.

57. Ho, K. S.; Poon, P. C.; Owen, S. C.; Shoichet, M. S., Blood vessel hyperpermeability and pathophysiology in human tumour xenograft models of breast cancer: a comparison of ectopic and orthotopic tumours. *BMC Cancer* **2012**, 12, 1-10.

58. Tannock, I. F.; Rotin, D., Acid pH in Tumors and Its Potential for Therapeutic Exploitation. *Cancer Research* **1989**, 49, 4373-4384.

59. Kato, Y.; Ozawa, S.; Miyamoto, C.; Maehata, Y.; Suzuki, A.; Maeda, T.; Baba, Y., Acidic extracellular microenvironment and cancer. *Cancer Cell International* **2013**, 13, 89-89.

60. Vogel, C. L.; Cobleigh, M. A.; Tripathy, D.; Gutheil, J. C.; Harris, L. N.; Fehrenbacher, L.; Slamon, D. J.; Murphy, M.; Novotny, W. F.; Burchmore, M.; Shak, S.; Stewart, S. J.; Press, M., Efficacy and Safety of Trastuzumab as a Single Agent in First-Line Treatment of HER2-Overexpressing Metastatic Breast Cancer. *Journal of Clinical Oncology* **2002**, 20, 719-726.

61. Bullock, K.; Blackwell, K., Clinical Efficacy of Taxane–Trastuzumab Combination Regimens for HER-2–Positive Metastatic Breast Cancer. *The Oncologist* **2008**, 13, 515-525.

62. Verma, S.; Miles, D.; Gianni, L.; Krop, I. E.; Welslau, M.; Baselga, J.; Pegram, M.; Oh, D.-Y.; Diéras, V.; Guardino, E.; Fang, L.; Lu, M. W.; Olsen, S.; Blackwell, K., Trastuzumab Emtansine for HER2-Positive Advanced Breast Cancer. *New England Journal of Medicine* **2012**, 367, 1783-1791.

II. POLYMER COATING ON Au-Fe_3O_4 NANOPARTICLES

ABSTRACT

Nanoparticle synthesizing methods have been widely studied for cancer treatment. However, aggregation of nanoparticles inside the blood vessel remains a problem for cancer treatment. The aggregation of the nanoparticles inside the vessel reduces the potential and ability of the nanoparticles by blocking access to the targeted site and removing them from the body. Here, we report a simple and fast method to solve the problem by depositing a thin layer of biocompatible polymers on the surface of nanoparticles to reduce the chance of collision of the nanoparticles, which will prevent them from aggregation. The thin layer (1.81 ± 0.60 nm) of poly-l-lysine (PLL) and polyethylene glycol (PEG) was deposited on Au-Fe_3O_4 nanoparticles. The average size of the nanoparticles was 58.27 ± 7.48 nm. The nanoparticles were uptaken by the breast cancer cells. The Au-Fe_3O_4 nanoparticles showed the toxicity to the breast cancer cells at 500 µg/ml. The NIR laser with Au-Fe_3O_4 nanoparticles was able to induce the hyperthermia effect to cells. These results suggest the optimal concentration of Au-Fe_3O_4 nanoparticles and the coating method to use in breast cancer treatment using the hyperthermia effect.

1. INTRODUCTION

Current cancer treatment methods have been focusing on noninvasive techniques. One of the interesting approaches is the hyperthermia effect. The hyperthermia effect occurs when the temperature is in the range of 39-42 ^{o}C for at least 1 hour.[18] At this temperature range, the effects (including inhibition of radiation that induces the damage repair, changes in perfusion, and re-oxygenation) are able to improve the therapy in the tumor sites.[19] One approach to the method of inducing hyperthermia effect is delivering metal nanoparticles to the tumor site. Gold nanoparticles have been studied due to their biocompatibility to the human body and cost-effective approach for cancer treatment.[20] Surface plasmon resonance (SPR) is the phenomenon that the electromagnetic field at a certain wavelength stimulates the free electrons across the surface of gold nanoparticles. As a result of SPR, the particles released the heat after they absorbed the electromagnetic field.[21] Various types of gold nanoparticles have been synthesized and used for hyperthermia-inducing therapy, such as gold nanoshells,[22] gold nanorods,[23] and gold nanospheres.[24] Near Infrared (NIR) wavelength (800-1300 nm) plays an important role in order to induce the SPR of gold nanoparticles because gold nanoparticles highly absorb the wavelength in this region.[25]

Even though gold nanoparticles were found useful for cancer treatment, there is still a drawback to this method. The disadvantage is the low retention time, as nanoparticles started to accumulate in the tumor site at high concentration.[26] In order to solve this problem, we coated the surface of the gold nanoparticle with biocompatible polymer PLL and PEG to prevent them from aggregation. PLL is the biocompatible cationic polymer that provides active amino groups that are useful for drug delivery and cell adhesion.[27]

Coating PLL on the surface of metal nanoparticles resulted in increased retention time of silver nanoparticles.[28] PEG is a neutral polyether, which is water soluble and has an ability to form two phases with other polymers. In addition, this polymer is non-toxic to cells.[29]

In this study, we coated Au-Fe_3O_4 nanoparticles with PLL together with PEG to create a polymer layer around the gold nanoparticles. We hypothesize that coating polymer on the surface of these nanoparticles will result in increased the retention time and prevention from aggregation, which would help increase the therapeutic efficacy for cancer treatment.

2. MATERIALS AND METHODS

2.1 PLL COATING ON Au-Fe_3O_4 NANOPARTICLES

All reagents were purchased from Sigma-Aldrich unless otherwise specified. Briefly, 25 mg/ml of bare gold nanoparticles was prepared in 1 ml of water. Then, 653 µL of 0.1% w/v of PLL was added to nanoparticles. After 1 minute of mixing, 250 µl of 1% w/v PEG was added to the mixture per 10 ml of mixture. The whole suspension was stirred for 5 minutes. The excess PLL and PEG were removed by centrifuging at 5,000 rcf for 30 minutes. The amount of PLL was quantified using Trypan Blue assay, which was modified from Grotzky *et al*.[30]

2.2 PLL- Au-Fe_3O_4 NANOPARTICLE CHARACTERIZATION

The morphology and size of nanoparticles were characterized by using a transmission electron microscope (TEM, Tecnai F20) at an accelerating voltage of 120 kV. A drop of 10 µl of sample was air-dried in carbon coated copper nanogrid (Tedpella). The size of Au-Fe3O4 and polymer coating thickness were measured using ImageJ (version 1.45S, NIH, USA).

2.3 BT-474 CELL CYTOTOXICITY WITH Au-Fe_3O_4 NANOPARTICLES

To estimate the optimal concentration of Au-Fe_3O_4 nanoparticles, BT-474 cells were cultured in Hybri-Care (ATCC) media supplemented with 10% Fetal Bobine Serum (FBS) and 1% (100 units/ml) Pennicillin-Streptpmycin (Corning) at 37 ^oC and 5% CO_2 respectively. Then, cells were plated in a 96- tissue culture well plate at a density of 10,000 cells per well in 200 µl of media. After 18 hours of growth, Au-Fe_3O_4 nanoparticles were

added to the medium. The final concentrations of Au-Fe_3O_4 nanoparticles were 500, 100, 50, 10, 5 and 1 µg/ml. The media was replaced to remove non-uptaken nanoparticles after 3 hours of incubation. After 72 hours, the plate was centrifuged down at 100 rcf for 15 minutes. The supernatant was discarded. Live cells were stained with 2 µM of Calcein AM (Life technologies) in PBS. The percentage of dead cells was calculated using equation 1.

$$\%\ inihibition\ in\ cell\ growth = \frac{F.I._{PBS\ treated\ cells} - F.I._{samples}}{F.I._{PBS\ treated\ cells}} \times 100. \quad (1)$$

In order to examine the cell apoptosis effects induced by PLL-coated gold nanoparticles, BT-474 cells were incubated with PLL-coated gold nanoparticles for 3 hours at 37 ^{o}C in a 96-tissue culture well plate. After the incubation, the cells were washed with sterilized PBS three times to remove non-uptaken nanoparticles.

2.4 *IN VITRO* CELL APOPTOSIS STUDY

The apoptosis study of PLL-coated gold nanoparticles was evaluated using HER2+ breast cancer cell line (ATCC). The cells were plated in a 96-tissue culture well plate at a density of 10,000 cells per well in 200 µl of media. After 18 hours of growth, 10 µl of PLL-coated gold nanoparticles was added to the medium. The final concentrations of PLL-coated nanoparticles were 100, 50, 10, 5 and 1 µg/ml. The media was replaced with fresh media to remove the non-uptaken nanoparticles after 3 hours of incubation. Then, the cells were treated with a NIR wavelength laser (790 nm) at 1 W/cm^2 for 1 minute. After 72 hours, the plate was centrifuged down at 100 rcf for 15 minutes. The supernatant was discarded. Live cells were stained with 2 µM of Calcein AM (Life technologies) in PBS. The plate was then incubated at R.T. for 45 minutes. The fluorescent intensity (F.I.) was measured using 485/528 filters using a plate reader (BioTek Synergy 2).

RESULTS

3.1 CHARACTERIZATION OF PLL-Au-Fe_3O_4 NANOPARTICLES

Because the shape of Au-Fe_3O_4 nanoparticles is both hexagonal and square, the equivalent diameter was used to measure the size of nanoparticles. The equivalent diameter of Au-Fe_3O_4 nanoparticles is 58.27 ± 7.48 nm, as shown in Fig 3.1 (a), while the PLL-Au-Fe_3O_4 nanoparticles diameter is 60.56 ± 7.18 nm. The thickness of the PLL coating is 1.81 ± 0.60 nm as shown in Fig 3.1 (b).

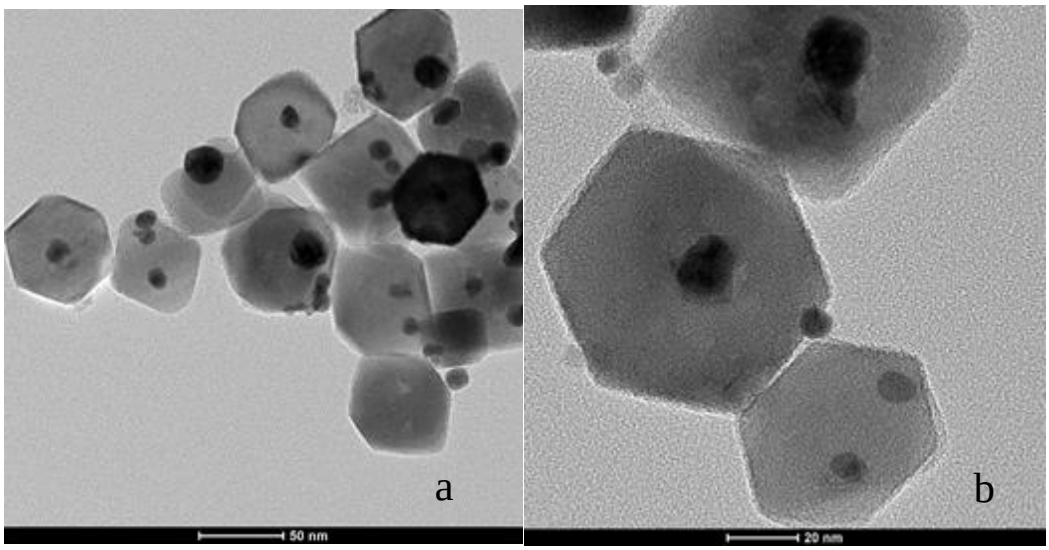

Figure 3.1 : TEM image of (a) uncoated Au-Fe_3O_4 nanoparticles. (b) PLL coating on Au-Fe_3O_4 nanoparticles.

3.2 CELLULAR UPTAKE OF Au-Fe_3O_4 NANOPARTICLES

Despite the size of Au-Fe_3O_4 nanoparticles, the intracellular uptake of Au-Fe_3O_4 nanoparticles were examined. The microscopic images confirmed the delivery of

nanoparticles inside the cells (Fig.3.2), indicating that the nanoparticles were uptaken inside the cells. No nanoparticles were found outside the cells.

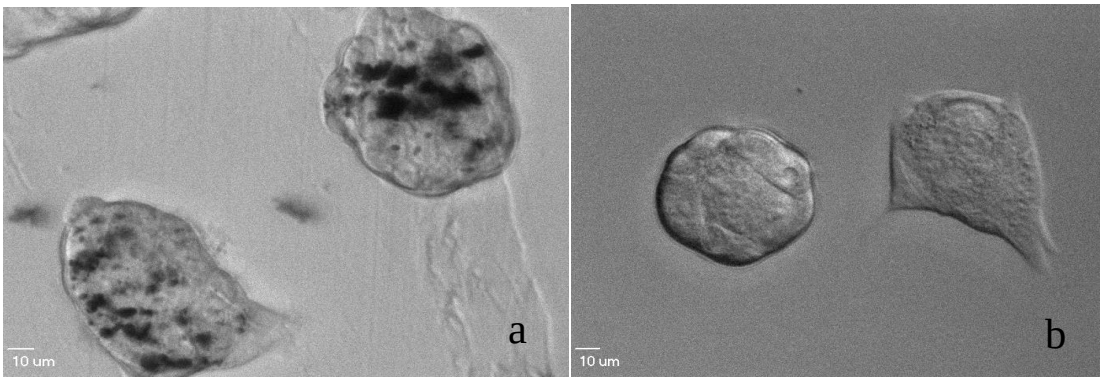

Figure 3.2 : Microscopic images of (a) Cellular uptake of 100 µg/ml of Au-Fe_3O_4 nanoparticles inside BT-474 cells. (b) PBS treated BT-474 cells

3.3 BT-474 CELL CYTOTOXICITY WITH Au-Fe_3O_4 NANOPARTICLES

According to Fig. 3.3, the Au-Fe_3O_4 nanoparticle at low concentration (up to 100 µg/ml) was found to have negligible cytotoxic effect to the cells, whereas the percentage of cell death increased to ~40% at 500 µg/ml, which might be the effect of the aggregation of nanoparticles.

3.4 EFFECTS OF THE Au-Fe3O4 NANOPARTICLE WITH NIR LASER TO BT-474 CELLS

After the optimal concentration of Au-Fe_3O_4 nanoparticles that did not cause cytotoxicity to BT-474 cells was known, the cells were incubated within that concentration. The cells were then exposed to NIR laser for 1 min. The results indicated that after the Au-Fe_3O_4 nanoparticles, uptaken cells were exposed to the laser, the percentage of death cells increased in every concentration, as shown in Fig. 3.4. The laser-PBS treated cells were

used as a control. The laser itself did not show toxicity to cells but the cells with the same concentration without using laser showed a negligible effect of toxicity to cells. For example, at 100 µg/ml of Au-Fe_3O_4 nanoparticles, the laser treated cells showed ~45% of

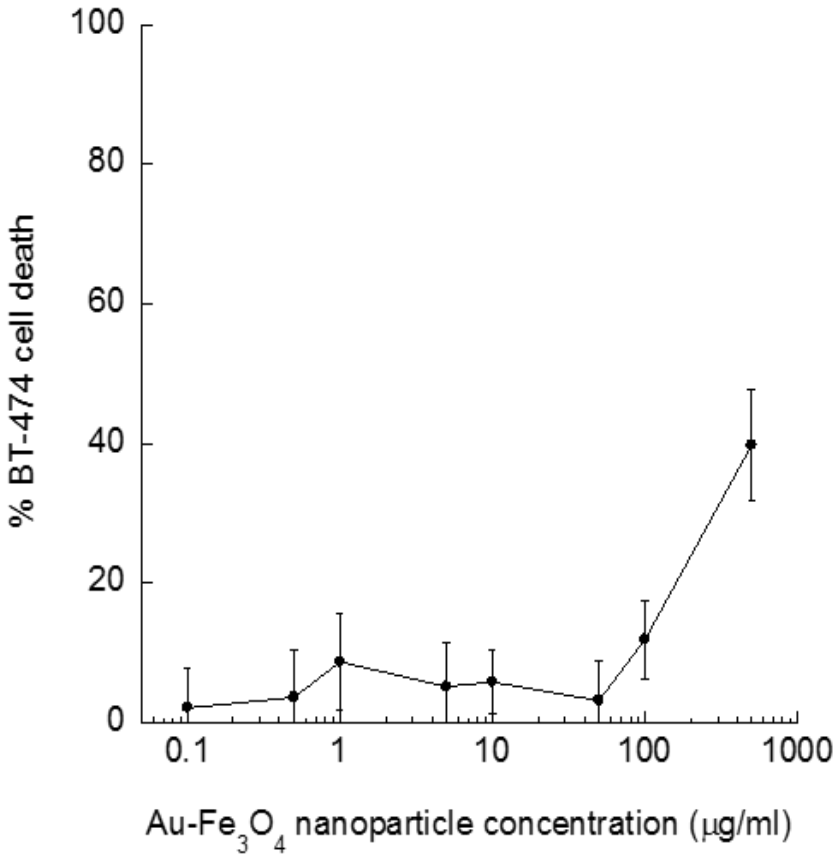

Figure 3.3: Au-Fe_3O_4 nanoparticle toxicity with BT-474 cells

cell death while non-laser treated cells showed only ~24% of cell death. The same trend also occurred at other concentrations of Au-Fe_3O_4 nanoparticles. This can be the evidence to confirm that the NIR laser can be used to induce the hyperthermia effect, which caused the cell death.

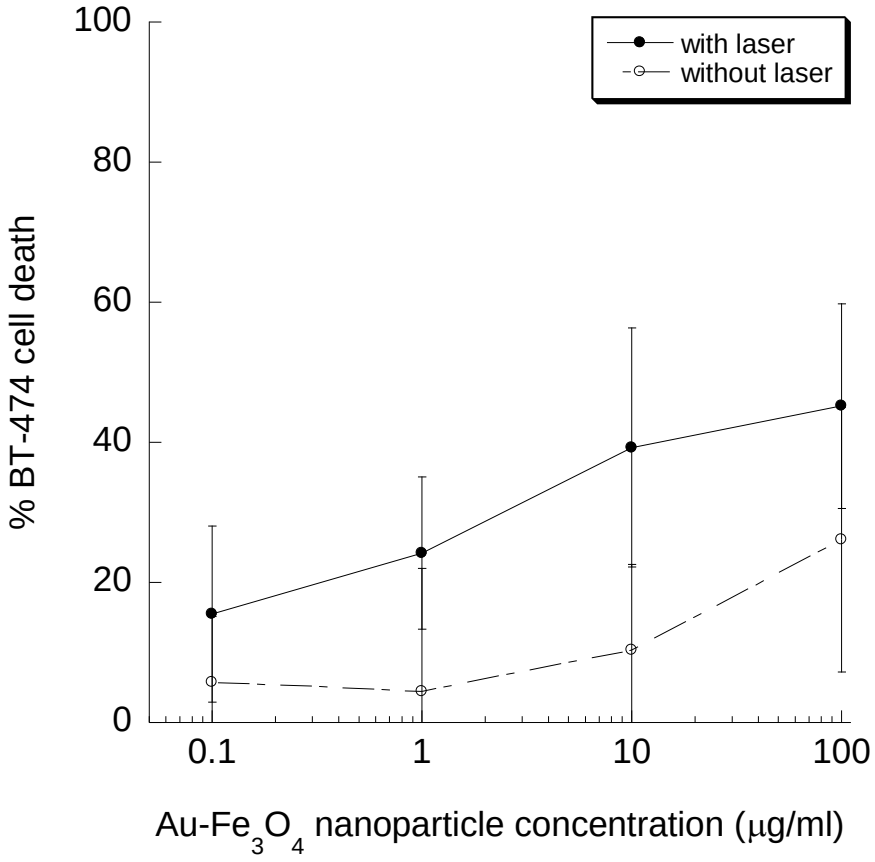

Figure 3.4: % BT-474 cell death after adding Au-Fe_3O_4 nanoparticles and exposing to NIR laser

4. DISCUSSION

The simple method to coat the surface of Au-Fe_3O_4 nanoparticles using both biopolymers, which are PLL and PEG was proposed. The particles themselves aggregated within the cells after they were uptaken by the cells. The microscopic images confirmed the cellular uptake of the nanoparticles. Most of the nanoparticles were found inside the cells. We also found that at the final concentration of 500 µg/ml, Au-Fe_3O_4 nanoparticles showed some cytotoxicity to BT-474 cells. This was due to nanoparticle aggregation. The NIR laser at 0.9-1.1 W/cm^2 for 10-15 minutes has been proved to maximize control of tumor growth in mice and minimize damage to surrounding cells.[31] It was also found that after exposing the cancer cell with NIR laser when incubated with Au nanorods, the efficacy of nanorods was intensified due to the increased efficiency of NIR absorption and photothermal conversion.[32] The hyperthermia effects, which increased the temperature to 41.5 ^oC, could be induced by exposing the NIR laser on the gold nanoparticles in the mice, which finally decreased the tumor volume.[33] Moreover, the apoptosis of cancer cells was also found to be evident after a combination of using the NIR laser at 1 W/cm^2 and gold nanoparticles.[34] The results indicated that after using the NIR laser on the cells with Au-Fe_3O_4 nanoparticles, they can increase the cell death due to the hyperthermia effects. However, these nanoparticles need specific targeting ability to reach the tumor site because some nanoparticles were found in other organs from *in vivo* studies.[33]

5. CONCLUSION

We have developed a fast and simple technique to coat the surface using biopolymers. The thin layer (1.81 ± 0.60 nm) of biopolymer was deposited on the surface of Au-Fe_3O_4 nanoparticles. The nanoparticles were uptaken inside the cells. At high concentration of Au-Fe_3O_4 nanoparticles at 500 µg/ml, the percentage of dead cells increased, which indicated the cytotoxic effect of these nanoparticles. In contrast, there was negligible cytotoxic effect to the cells at lower concentrations. The uncoated Au-Fe_3O_4 nanoparticles were able to use for cancer treatment by inducing hyperthermia effects to cells after exposing the cell with Au-Fe_3O_4 nanoparticles with NIR laser. These results recommend the optimal concentrations of using the Au-Fe_3O_4 nanoparticles to use in the study of induced hyperthermia effects for cancer therapy and show that our Au-Fe_3O_4 nanoparticles can be used to treat the cancer by inducing hyperthermia effects to cancer cells. However, future studies are needed, including studies on the stability study of the nanoparticles, the amount of each polymer quantification, and *in vitro* studies of hyperthermia effect.

SECTION

2. CONCLUSIONS AND FUTURE WORKS

In this study, polymer-coated anticancer drug-encapsulated NRs were prepared by the solvent diffusion method. The mean size of PCL-coated CPT NRs was 500.9 ± 91.3 nm in length and 122.7 ± 10.1 nm in width. The anticancer drug-encapsulated NRs have the ability to degrade in the acidic environment present in tumor sites. Then, the released drug diffuses into the pores of the polymer and then into cancer cells. In this study, the conjugation of TTZ on NRs enabled the NRs to specifically target only the breast cancer cells. It was found that the specific targeting anticancer drug-encapsulated NRs significantly inhibited the BT-474 breast cancer cell growth. Although *in vitro* studies showed high possibility to inhibit breast cancer cell growth, this study still needs evidence from *in vivo* studies for therapeutic efficacy.

In addition, biopolymer coating on the surface of Au-Fe_3O_4 nanoparticles is one technique to solve the aggregation problem of these nanoparticles. Coating biopolymer on nanoparticles provide advantages for biomedical applications, especially for drug delivery. Therefore, the study of coating polymer on nanoparticles rather than using the drug as drug-encapsulated nanoparticles might be able to increase the potential of nanoparticles such as gold nanoparticles, which are used in early detection of cancers and cancer therapy. The study showed the feasibility study of using Au-Fe_3O_4 nanoparticles with the principal of thermal therapy; however, the further studies are needed for more evidence, such as the quantification of PLL and PEG on the surface of nanoparticles, *in vitro* studies of using NIR laser to induce cell apoptosis by the hyperthermia effect, and *in vivo* studies for treatment efficacy.

BIBLIOGRAPHY

1. Coates, A.; Abraham, S.; Kaye, S. B.; Sowerbutts, T.; Frewin, C.; Fox, R.; Tattersall, M., On the receiving end—patient perception of the side-effects of cancer chemotherapy. *European Journal of Cancer and Clinical Oncology* **1983,** *19* (2), 203-208.

2. Hotze, E. M.; Phenrat, T.; Lowry, G. V., Nanoparticle aggregation: challenges to understanding transport and reactivity in the environment. *Journal of environmental quality* **2010,** *39* (6), 1909-1924.

3. Kweon, H.; Yoo, M. K.; Park, I. K.; Kim, T. H.; Lee, H. C.; Lee, H.-S.; Oh, J.-S.; Akaike, T.; Cho, C.-S., A novel degradable polycaprolactone networks for tissue engineering. *Biomaterials* **2003,** *24* (5), 801-808.

4. Woodruff, M. A.; Hutmacher, D. W., The return of a forgotten polymer—polycaprolactone in the 21st century. *Progress in Polymer Science* **2010,** *35* (10), 1217-1256.

5. Ortiz, R.; Prados, J.; Melguizo, C.; Arias, J. L.; Ruiz, M. A.; Alvarez, P. J.; Caba, O.; Luque, R.; Segura, A.; Aranega, A., 5-Fluorouracil-loaded poly (ε-caprolactone) nanoparticles combined with phage E gene therapy as a new strategy against colon cancer. *International journal of nanomedicine* **2012**.

6. Makadia, H. K.; Siegel, S. J., Poly lactic-co-glycolic acid (PLGA) as biodegradable controlled drug delivery carrier. *Polymers* **2011,** *3* (3), 1377-1397.

7. Farazuddin, M.; Sharma, B.; Khan, A. A.; Joshi, B.; Owais, M., Anticancer efficacy of perillyl alcohol-bearing PLGA microparticles. *International journal of nanomedicine* **2012,** *7*, 35.

8. Verderio, P.; Bonetti, P.; Colombo, M.; Pandolfi, L.; Prosperi, D., Intracellular drug release from curcumin-loaded PLGA nanoparticles induces G2/M block in breast cancer cells. *Biomacromolecules* **2013,** *14* (3), 672-682.

9. Garlotta, D., A literature review of poly (lactic acid). *Journal of Polymers and the Environment* **2001,** *9* (2), 63-84.

10. Yu, L.; Dean, K.; Li, L., Polymer blends and composites from renewable resources. *Progress in polymer science* **2006,** *31* (6), 576-602.

11. Zhu, D.; Tao, W.; Zhang, H.; Liu, G.; Wang, T.; Zhang, L.; Zeng, X.; Mei, L., Docetaxel (DTX)-loaded polydopamine-modified TPGS-PLA nanoparticles as a targeted drug delivery system for the treatment of liver cancer. *Acta biomaterialia* **2016,** *30*, 144-154.

12. Jiang, D.; Gao, X.; Kang, T.; Feng, X.; Yao, J.; Yang, M.; Jing, Y.; Zhu, Q.; Feng, J.; Chen, J., Actively targeting D-α-tocopheryl polyethylene glycol 1000 succinate-poly (lactic acid) nanoparticles as vesicles for chemo-photodynamic combination therapy of doxorubicin-resistant breast cancer. *Nanoscale* **2016,** *8* (5), 3100-3118.

13. Nitta, S. K.; Numata, K., Biopolymer-based nanoparticles for drug/gene delivery and tissue engineering. *International journal of molecular sciences* **2013,** *14* (1), 1629-1654.

14. Zhang, Y.; Wang, H.; Mukerabigwi, J. F.; Liu, M.; Luo, S.; Lei, S.; Cao, Y.; Huang, X.; He, H., Self-organized nanoparticle drug delivery systems from a folate-targeted dextran–doxorubicin conjugate loaded with doxorubicin against multidrug resistance. *RSC Advances* **2015,** *5* (87), 71164-71173.

15. Esposito, E.; Cortesi, R.; Nastruzzi, C., Gelatin microspheres: influence of preparation parameters and thermal treatment on chemico-physical and biopharmaceutical properties. *Biomaterials* **1996,** *17* (20), 2009-2020.

16. Lu, Z.; Yeh, T.-K.; Tsai, M.; Au, J. L.-S.; Wientjes, M. G., Paclitaxel-loaded gelatin nanoparticles for intravesical bladder cancer therapy. *Clinical Cancer Research* **2004,** *10* (22), 7677-7684.

17. Li, W.-M.; Chiang, C.-S.; Huang, W.-C.; Su, C.-W.; Chiang, M.-Y.; Chen, J.-Y.; Chen, S.-Y., Amifostine-conjugated pH-sensitive calcium phosphate-covered magnetic-amphiphilic gelatin nanoparticles for controlled intracellular dual drug release for dual-targeting in HER-2-overexpressing breast cancer. *Journal of Controlled Release* **2015,** *220*, 107-118.

18. Dewhirst, M.; Viglianti, B.; Lora-Michiels, M.; Hanson, M.; Hoopes, P., Basic principles of thermal dosimetry and thermal thresholds for tissue damage from hyperthermia. *International Journal of Hyperthermia* **2003,** *19* (3), 267-294.

19. Dewhirst, M. W.; Vujaskovic, Z.; Jones, E.; Thrall, D., Re-setting the biologic rationale for thermal therapy. *International Journal of Hyperthermia* **2005,** *21* (8), 779-790.

20. Mukherjee, S.; Sau, S.; Madhuri, D.; Bollu, V. S.; Madhusudana, K.; Sreedhar, B.; Banerjee, R.; Patra, C. R., Green synthesis and characterization of monodispersed gold nanoparticles: toxicity study, delivery of doxorubicin and its bio-distribution in mouse model. *Journal of Biomedical Nanotechnology* **2016,** *12* (1), 165-181.

21. Li, J.-L.; Gu, M., Gold-nanoparticle-enhanced cancer photothermal therapy. *IEEE Journal of selected topics in quantum electronics* **2010,** *16* (4), 989-996.

22. Loo, C.; Lin, A.; Hirsch, L.; Lee, M.-H.; Barton, J.; Halas, N.; West, J.; Drezek, R., Nanoshell-enabled photonics-based imaging and therapy of cancer. *Technology in cancer research & treatment* **2004,** *3* (1), 33-40.

23. Huff, T. B.; Tong, L.; Zhao, Y.; Hansen, M. N.; Cheng, J.-X.; Wei, A., Hyperthermic effects of gold nanorods on tumor cells. **2007**.

24. Pitsillides, C. M.; Joe, E. K.; Wei, X.; Anderson, R. R.; Lin, C. P., Selective cell targeting with light-absorbing microparticles and nanoparticles. *Biophysical journal* **2003,** *84* (6), 4023-4032.

25. Liu, H.; Chen, D.; Tang, F.; Du, G.; Li, L.; Meng, X.; Liang, W.; Zhang, Y.; Teng, X.; Li, Y., Photothermal therapy of Lewis lung carcinoma in mice using gold nanoshells on carboxylated polystyrene spheres. *Nanotechnology* **2008,** *19* (45), 455101.

26. Matsumura, Y.; Maeda, H., A new concept for macromolecular therapeutics in cancer chemotherapy: mechanism of tumoritropic accumulation of proteins and the antitumor agent smancs. *Cancer research* **1986,** *46* (12 Part 1), 6387-6392.

27. Shan, C.; Yang, H.; Han, D.; Zhang, Q.; Ivaska, A.; Niu, L., Water-soluble graphene covalently functionalized by biocompatible poly-L-lysine. *Langmuir* **2009,** *25* (20), 12030-12033.

28. Marsich, L.; Bonifacio, A.; Mandal, S.; Krol, S.; Beleites, C.; Sergo, V., Poly-L-lysine-coated silver nanoparticles as positively charged substrates for surface-enhanced Raman scattering. *Langmuir* **2012,** *28* (37), 13166-13171.

29. Harris, J. M., *Poly (ethylene glycol) chemistry: biotechnical and biomedical applications*. Springer Science & Business Media: 2013.

30. Grotzky, A.; Manaka, Y.; Fornera, S.; Willeke, M.; Walde, P., Quantification of α-polylysine: a comparison of four UV/Vis spectrophotometric methods. *Analytical Methods* **2010,** *2* (10), 1448-1455.

31. Dickerson, E. B.; Dreaden, E. C.; Huang, X.; El-Sayed, I. H.; Chu, H.; Pushpanketh, S.; McDonald, J. F.; El-Sayed, M. A., Gold nanorod assisted near-infrared plasmonic photothermal therapy (PPTT) of squamous cell carcinoma in mice. *Cancer letters* **2008,** *269* (1), 57-66.

32. Tong, L.; Zhao, Y.; Huff, T. B.; Hansen, M. N.; Wei, A.; Cheng, J. X., Gold nanorods mediate tumor cell death by compromising membrane integrity. *Advanced Materials* **2007,** *19* (20), 3136-3141.

33. Glazer, E. S.; Zhu, C.; Massey, K. L.; Thompson, C. S.; Kaluarachchi, W. D.; Hamir, A. N.; Curley, S. A., Noninvasive radiofrequency field destruction of pancreatic adenocarcinoma xenografts treated with targeted gold nanoparticles. *Clinical Cancer Research* **2010,** *16* (23), 5712-5721.

34. Hauck, T. S.; Jennings, T. L.; Yatsenko, T.; Kumaradas, J. C.; Chan, W. C., Enhancing the toxicity of cancer chemotherapeutics with gold nanorod hyperthermia. *Advanced Materials* **2008,** *20* (20), 3832-3838.

VITA

Tunyaboon Laemthong received his Bachelor of Engineering in Chemical Engineering at Kasetsart University, Thailand in March 2013. During his senior year, he worked on the project entitled "Feasibility study of the cultivation of *Rhodococcus opacus* PD630 from dairy waste". He joined Dr. Barua's group in May 2015 in the Department of Chemical and Biochemical Engineering at Missouri University of Science and Technology.

During his course of study, he worked on synthesis, characterization and *in vitro* studies of biopolymer coating on nanoparticles. In December 2016, he received his Master's degree in Chemical Engineering at Missouri University of Science and Technology.